N70-38721

NASA SP-8026

NASA
SPACE VEHICLE
DESIGN CRITERIA
(GUIDANCE AND CONTROL)

SPACECRAFT STAR TRACKERS

JULY 1970

NATIONAL AERONAUTICS AND SPACE ADMINISTRATION

FOREWORD

NASA experience has indicated the need for uniform criteria for the design of space vehicles. Accordingly, criteria are being developed for the following areas of spacecraft technology:

Environment
Structure
Guidance and Control
Chemical Propulsion

Individual components of this work will be issued as separate monographs as soon as they are completed. This document, "Spacecraft Star Trackers," is one such monograph. A list of all published monographs in the series can be found in the back of this document.

These monographs are to be regarded as guides to design and not as NASA requirements, except as may be specified in formal project specifications. It is expected, however, that the criteria sections of these monographs, revised as experience may dictate, eventually will become uniformly applied to the design of NASA space vehicles.

This monograph was prepared by the Kollsman Instrument Corp. under the cognizance of the NASA Electronics Research Center. The effort was guided by an advisory panel chaired by Louis E. Sharpe of Kollsman Instrument Corp. The following individuals participated in the advisory panel activities:

J. Bebris	NASA Electronics Research Center
R. F. Bohling	NASA Office of Advanced Research and Technology
F. J. Carroll	NASA Electronics Research Center
R. L. Cleavinger	Ball Brothers Research Corp.
T. P. Dixon	ITT Aerospace
C. D. Engel	NASA Langley Research Center
F. F. Forbes	University of Arizona
K. V. Knight	Litton Systems, Inc.
A. R. Leslie	Kollsman Instrument Corp.
F. D. MacKenzie	NASA Electronics Research Center
J. M. McLauchlan	Jet Propulsion Laboratory
T. S. Michaels	NASA Office of Advanced Research and Technology
G. R. Quasius	General Electric Corp.

Comments concerning the technical contents of these monographs will be welcomed by the National Aeronautics and Space Administration, Office of Advanced Research and Technology (Code RVA), Washington, D.C. 20546.

July, 1970

For sale by the Clearinghouse for Federal Scientific and Technical Information
Springfield, Virginia 22151 – Price $3.00

CONTENTS

Spacecraft Star Trackers

1. INTRODUCTION

Star sensing and tracking devices have been developed for a variety of spacecraft applications in which the determination of a known reference direction is required for vehicle attitude control and for the generation of navigation and guidance data.

Star-tracker system design is dominated by the low power level of starlight in the presence of extraneous light sources and system noise. Other factors influencing design are requirements for high accuracy, low weight, low power drain, and survival during launch and in the space environment.

The preferred approach to the design of a spaceborne star tracker is one that efficiently concentrates the star energy into a small image and, by preferential sensing, recognizes and registers the presence of such an image relative to a central point in the field of observation. The resulting measures of presence and pointing error are separated electronically, the first being used for star verification (and often for automatic gain control (AGC)) and the second for tracking control.

In equipment design, lightweight and compact optical systems, field scan systems that minimize mechanical friction, and solid-state circuitry generally are preferred.

Degraded performance or equipment failure can result from designs based on an incorrect appraisal of mission and vehicle constraints or from an incomplete knowledge of the operational environment. Examples of difficulties encountered include the tracking of stray light, arcing of high-voltage circuits, and development of index error from internal mechanical, electronic, and magnetic shifts.

The scope of this monograph is limited to star trackers. It considers that part of the tracking system that collects, scans, and senses the star and electronically derives a measure of star position relative to an optical reference. The error signal may be used to close an electronic tracking loop within the scanner or may be used for the control of supporting gimbals or the spacecraft. Orientation servomechanisms, output angle transducers, and computational elements relating to navigation and guidance are not discussed.

2. STATE OF THE ART

2.1 Evolution

Prior to 1946, a few star-tracking devices had been designed for telescope pointing control in large observatories (ref. 1). Although not applicable to a space environment, these early forms incorporated most of the essentials of star-tracker system design. Available components were primitive by current standards. However, a practicable low-noise, high-gain photodetector had become available as a stock item in the form of the multiplier phototube (ref. 2). This component served as the most used star sensor for the next two decades (1946 to 1966).

The state of the art in the 1950 to 1960 era was largely exemplified by systems having photomultiplier sensors and employing components such as motors, gear trains, synchros, and mechanically rotating shutters and rasters. Electronic circuits used vacuum tubes and discrete components. Applications were confined to aircraft (B-52, B-57, B47, B-58) (ref. 3) and missiles (SNARK [ref. 4] and Hound Dog) in which star directions were used to obtain star altitude for position fixing and star bearing for true heading determination.

Design efforts to improve these systems were aimed primarily at increasing their accuracy from minutes to seconds of arc and at the development of a capability for tracking stars through the sunlit Earth's atmosphere. Solid-state sensors were introduced in this period as a potential solution to the problem of discrimination against daylight. Efforts to improve reliability were somewhat limited by the inherent complexity of the equipment and of interface requirements with inertial systems. The reliability levels required for forthcoming space applications were not consistent with the few-hundred-hour mean time between failures (MTBF) typical of the airborne systems. The space applications specified a high probability of successful operation during mission times of 2000 to 6000 hr.

The first attempt to operate a star tracker from a vantage point above the Earth's atmosphere was made in 1959 by Johns Hopkins Applied Physics Laboratory in connection with the balloon-borne Venus experiment known as Stratolab High (ref. 5). This demonstration of a planet-oriented fine pointing system was followed in the next 8 years by other balloon-borne experiments–Bal-Ast (Johns Hopkins) (ref. 6), Stratoscope II (Princeton) (ref. 7), and Polariscope (Univ. of Arizona) (ref. 8)–in which planet- and star-oriented trackers were used.

In the same period, various rocket-borne experiments were undertaken by Goddard Space Flight Center, Kitt Peak National Observatory, and USAF, in which star trackers were borne aloft in a trajectory that became ballistic after burnout. These designs required survival of the launch experience and operation in a near vacuum. The period of operation in this environment was brief.

Star trackers for extended operation in space appeared with such programs as Mariner, Surveyor, Lunar Orbiter, and Orbiting Astronomical Observatory (OAO). Each of these programs called for a star-tracker design tailored specifically to its spacecraft and mission.

2.2 Basic Principles of the System

The basic principle by which balloon, rocket, and spaceborne equipment perform their function is the same, although the means of implementation differ. As suggested by figure 1, the energy of a target star is collected by a set of optics and brought to focus for electronic scanning or mechanical modulation. A photodetector then transduces the modulated star energy into an electrical signal that contains information on star presence (or relative brightness) and the angle of the star direction relative to the optical axis. The latter is used as a tracking signal.

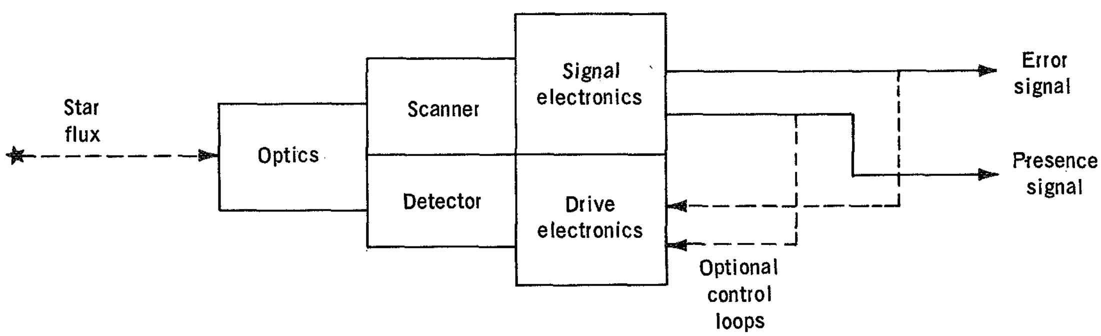

Figure 1.—Functional subsections of star tracker.

In the tracking systems on Mariner and Lunar Orbiter, electronic deflection served to null the track signal anywhere in the field of view. In the OAO tracker, nulling was done with a photomultiplier by means of torque-driven gimbals, imposing more moving parts but allowing a much larger solid angle of operation. Surveyor, with its photomultiplier system, achieved tracking null by roll of the spacecraft, thereby avoiding both mechanical gimbals and electronic positioning of its field of view.

Design practice for spaceborne star-tracking systems has evolved a number of parameters. For convenience, operational parameters, which characterize the needs of the application, are here separated from design parameters, which are chosen to satisfy the specified operation.

Operational parameters:

(1) Number of stars and preferred directions
(2) Search area
(3) Search time
(4) Acquisition probability
(5) Tracking accuracy
(6) Stray-light environment (position of Sun, Earth, etc.)
(7) Response to error signal (operational tracking bandwidth, angular velocity, and angular acceleration)
(8) Shock and vibration
(9) Thermal environment

Design parameters:

(1) Minimum star flux
(2) Working field of view (FOV)
(3) Acquisition FOV
(4) Acquisition time
(5) Acquisition signal-to-noise (S/N) ratio
(6) Star acceptance criteria
(7) Noise equivalent angle
(8) System bandwidth
(9) Detector response
(10) Optical aperture, focal length, transmission
(11) Stray-light suppression factors
(12) Stiffness, balance, etc.
(13) Thermal design parameters

2.3 Comparison of Recent Tracking Systems

Although star-tracker designs may differ greatly in their implementation of the tracking principle, it will be useful to compare the design and performance differences that exist between systems designed for the same function. For this purpose, most of the systems representing the state of the art in the 1960's can be grouped into four functional categories:

(1) Canopus trackers have unique target star in terms of both appearance and use.
(2) Rocket-borne trackers operate in ballistic trajectory.
(3) Gimbaled star trackers must operate on any one of a specific set of guide stars.
(4) Fine-guidance trackers have optics boresighted to a given experiment or related optical system.

Specific values for parameters of tracking systems representing these categories are given in table I. All have been built and tested, and most have been flown. The following sections discuss each group in more detail and review some instructive experiences encountered during the design, test, and flight phases of the associated space programs.

2.4 Canopus Tracker

The unique location of the bright star Canopus near the southern pole of the ecliptic plane (14°) makes it especially useful as a reference direction for the determination of roll attitude about the sun line. Also, for trajectories in the ecliptic plane, and Sun is always at nearly right angles to Canopus, thereby simplifying the problem of shielding. A Sun/Canopus attitude reference system based upon these advantages has been used for the orientation of midcourse guidance corrections of Mariner, Surveyer, and Lunar Orbiter.

The Canopus tracker must be able to acquire its star during a roll search in which the stars from an entire great circle belt on the celestial sphere may pass through the acquisition FOV. At any given time, the sequence of stars and planets in this belt is known. Successful acquisition of Canopus has been obtained on all flights by comparing this known sequence with the sequence of tracker responses telemetered from the spacecraft during roll. The process is referred to as roll mapping. Some success has been achieved also in acquiring Canopus by brightness gates alone.

In the Canopus tracker for Surveyor, a 1P21 photomultiplier was used to detect the star energy after mechanical chopping by a rotating spoked raster. On Mariner and Lunar Orbiter, an image dissector was used to track the image of Canopus electronically on its photocathode. Useful experience gained from the Canopus tracker programs follow.

2.4.1 Mariner

The Canopus tracker functioned successfully on both the Mariner 4 and the 5 flights (refs. 9, 10, and 11). In the case of Mariner 4, the tracker functioned throughout the 3 years of vehicle operation, setting a high mark in the state of the art for operational life.

During periods of active roll search, the technique of ground-based roll-map matching was successfully used for identification of stars. Telemetered brightness measurements from the sensor were compared with prior computations. Unique stars and bright portions of sky, such as the Milky Way, were identified in real time as Mariner rolled in search of the star Canopus.

TABLE I.–*Comparison of*

Vehicle	Canopus trackers			Gimbaled
	Mariner 4	Lunar Orbiter	Surveyor	OAO
Tracker volume		12 X 5.5 X 4 in.	180 in.^{3}	17.5 X 11 X 16.25 in.
Electronics volume				16 X 11 X 4
Weight	5 lb	7.5 lb		43 lb
Power	1.5 W	3.5 W	5.0 W	15 W
Mechanical gimbals	None	1 preset	1 preset	2 axes
Gimbal angle	---	±8.75° yaw	±15°	±43° each
Instantaneous FOV	.85° roll by 11°	1° roll by 16°	.2° roll by 5°	25′ by 60′
Acquisition FOV	4° by 30°	8.2° roll by 16°	8° roll by 5°	1° by 1°
Track FOV	4° by 11°	8.2° roll by 16°	4° roll by 5°	1° by 1°
Working FOV	4° by 30°	8.2° roll by 33.5°	8° roll by 5°	1° by 1°
Number of stars	1	1	1	38
Min. star magnitude	Canopus	Canopus	Canopus	+2
Sun angle	≈70°	70°		32°
Earth/Moon angle	10°–25°	30°		14°
Optics	catadioptric	refractive	folded refractive	Newtonian
Aperture diameter	1.3 in.	2 cm	1 in.	3.5 in.
F/Number	.6	1	2	1.4
Focal length	.8 in.	2 cm		5.0 in.
Search area	30° by 360° roll	16° by 360° roll	5° by 360° roll	⩽ gimbal angle
Acquisition time		.25 sec		.25 sec
Track bandwidth	.312 Hz	1.8 Hz		1 Hz
Tracking time constant	.5 sec	.15 sec	1 sec	
Search rate	.116°/sec roll	4°/sec roll	.5°/sec roll	
Operational accuracy	6′	30″, 1σ	6′, 3σ	22″, 1σ
N.E.A.	20″, 1σ	15″, 1σ	4.2′ peak to peak	5″, 1σ
Scan/modulation	electrostatic	magnetic	mechanical	mechanical
Detector	Im. Diss./CBS S-11	Im. Diss./ITT S-20	1P21 RCA S-4	1P21 RCA S-4
Manufactured by	Barnes/JPL	ITT	Hughes	Kollsman

trackers	Rocket/missile trackers		Fine guidance	
USAF	Aerobee 150A	Aerobee 150A	OAO/GEP	OAO boresighted
14 X 8.5 X 8.5 in.	5 in. diam 10.5 in. length	4 in. diam 11 in. length	---	3 in. diam X 15 in. 5 X 11 X 12 in.
20 lb	9.5 lb	8.6 lb	15 lb	23 lb
12 W	8.5 W	6 W	2.6 W	7.7 W
2 axes	none	none	none	none
± 60° each	---	---	---	---
1° X 1°	16′ X 16′	20′ X 20′	1.5′	10′ diam
1° X 1°	8° diam	8° diam	4.5′ diam	20′ diam
1° X 1°	1° by 1° cross	1° by 1° cross	4.5′ diam	20′ diam
	8° diam	8° diam	4.5′ diam	180′ by 20′
100	153	1	400 000	4100
+2	+3	+1.0	+10	+6
25°	90°	>90°	45°	45°
13°		>90°	45°	25°
Mangin	refractive	refractive	Dall-Kirkham Ritchey-Chrétien	refractive
2.5 in.	5 cm	2.7 in.	8 in. effective	2.6 in.
1.2	1.5	.75	F/10 equiv	1.85
3 in.	7.5 cm	2 in.	53.2 in. equiv	4.85
⩽ gimbal angle	8° diam	8° diam	---	20′ diam
.5 sec	⩽ 1 sec		.5 sec	.1 sec
1 Hz	⩽45° lag at 5 Hz	10 Hz	3.5 Hz	.5 Hz
.5°/sec	4°/sec roll		---	.1°/sec
30″, 1σ	30″, 1σ	< 1′	.1″ to 5″	5″
5″, 1σ	12″, 1σ	10″	.1″ to 5″	1.6″
mechanical	magnetic	magnetic	mechanical	magnetic
Solid-state	Im. Diss./ITT	Im. Diss./ITT	PMT/EMR	Im. Diss./ITT
silicon	S-20	S-20	S-17	S-20
Kollsman	ITT	Ball Bros.	Kollsman	ITT

Sensitivity to scattering from off-axis earthshine was discovered in advance by test. Preventive measures included shielding, reduction of scattering by optics, and special acquisition logic. Remaining Earth response was used as part of the known roll map.

The false acquisition of spurious light sources was observed. Analysis indicated these sources to be sunlit dust particles dislodged from the solar paddle, possibly by meteroids.

Mariner 5 successfully flew by the planet Venus in October 1967 at an altitude of 4000 km from the surface at closest approach. During this time, a continuous lock on Canopus was maintained despite the severe stray light reflected from Venus (ref. 6).

2.4.2 Surveyor

A Canopus tracker was used successfully on all five completed missions and on incomplete mission 2 (refs. 12 and 13).

Simulation of Sun scattering helped to guide the development of baffles. In flight, however, an abnormally high dark-noise level during search was deemed qualitative evidence of residual stray-light input.

Some evidence of signal "spikes" during roll was attributed to sunlit particles from the helium vernier engine fired during midcourse.

Canopus signal levels exceeded expected values to the limiting point of the electronics. This effect was attributed in part to the difficulty of establishing test levels for star and sunlight that would be representative of their actual irradiance. This problem was solved for Surveyor 3, which achieved automatic recognition of Canopus for the first time in space.

Window fogging was experienced in solar thermal vacuum test, and the causative material (silicone grease) was identified and removed. This case illustrates the need for care when vacuum evaporable materials are used near optical surfaces.

Vibration testing proved the need for increased stiffness of electronic units.

Failure to lock on the minimum acceptable star level following environmental test was cured by selecting 1P21 tubes less sensitive to temperature variations.

Increased detector noise level was anticipated as a possibility when the vehicle passed through the outer edge of the Van Allen belt. No evidence of this effect was detected in flight, however.

2.4.3 Lunar Orbiter

On all five flights (refs. 14 and 15), the Canopus tracker was successfully employed as a reference for roll orientation.

False acquisition on Lunar Orbiter 1 and Lunar Orbiter 4 was experienced as a result of sunlight scattering off parts of the spacecraft, such as the solar panels and the omniantenna, and into the optics. Painting of offending surfaces did not completely solve the problem because of the residual reflectivity of black paint and the intensity of sunlight.

On Lunar Orbiter 2, normal operation was obtained during translunar flight in direct sunlight. However, Canopus was lost after injection into lunar orbit because of reflections of moonlight. Tracker operation was normal in the Moon's shadow.

During the Lunar Orbiter 3 translunar flight, Canopus was tracked steadily except for several dropouts, one associated with firing of the squibs and one with Moon albedo prior to lunar orbit injection.

Arcing at the high-voltage electronics was encountered during thermal vacuum tests as a result of partial pressures remaining before outgassing was complete. The problem was solved by introducing changes in circuit fabrication and insulation and by an increase in time before turnon in vacuum.

Image-dissector tubes were selected and tested for requirements specific to this application to guarantee in-flight performance. Some drop in output was observed after long exposures to star illumination or to excessive light from objects such as the Moon. This fatigue was observed to heal during the tracker OFF periods.

Use of a voltage regulator in the tracker eliminated the effect of changes in the space-vehicle power-supply output resulting from transitions between Sun and shadow in orbit.

2.5 Rocket-Borne Trackers

Star trackers capable of offset scanning have been used on Aerobee rocket probes as a reference for the attitude control of various astronomical experiment payloads. A series of 14 Aerobee 150A flights was successfully carried out by the Goddard Space Flight Center using an image dissector in the spinning probe. Stars to +3 mag were tracked. In a similar application, Kitt Peak National Observatory successfully used a despun tracker in an Aerobee 150 for planet pointing. Two flights were undertaken, one oriented on Venus and the other on Mars.

Successful designs for rocket-probe star trackers differ in some respects from those for orbiting spacecraft. The brief time allocated to payload orientation and operation calls for a relatively high value of star-detection rate.[1] Because the equipment was intended for operation at night, the absence of scattered sunlight allowed a design tradeoff in favor of detection rate. Also, the brevity of the probe trajectory in a spacelike environment eliminated the usual design concern over lubrication, long life, and ionizing radiation. The possibility of corona occurring at the high-voltage points of the image-dissector parts and circuitry required special precautions. In rocket-probe star trackers, this phenomenon was successfully suppressed.

A unique form of rocket-borne star tracker was used in a series of experiments by USAF (ref. 16). In this application, a vidicon was used as the star scanner and detector, featuring an off-axis electronic tracking capability similar to that of the image dissector. Ambient light from sunlit background was relatively high and, therefore, unrepresentative of most space-vehicle applications. To attain a high acquisition rate, the vidicon was physically stabilized to allow full use of the noise-integrating characteristics of its photoconductive image electrode.

As had been experienced with previous vidicon star trackers, this system exhibited a form of coherent noise resulting from the background illumination of hot spots on the image electrode. The number of spots was found to vary with temperature and to increase with tube use. At the time, remedial action called for mapping of the scan addresses of the hot spots to avoid their acceptance as false targets.

2.6 Gimbaled Star Trackers

In applications where the spacecraft must operate in a variety of attitudes with respect to spatial coordinates, the two-gimbal star tracker finds frequent application as a source for vehicle attitude reference.

This function is exemplified by the coarse-alinement star trackers of the OAO. Each of several trackers on the spacecraft is gimbaled to cover a working cone of approximately 90° apex angle. After acquiring any one of 38 guide stars, the star tracker develops error signals for gimbal restoration of the error to null. The error signals are developed by using orthogonally placed vibrating reeds to modulate the star image. The modulated energy is then sensed by a photomultiplier tube. A backup tracker, also developed for OAO coarse-alinement function, uses an image dissector for developing the gimbal nulling signals.

[1]For brightest star acquisition from Goddard's Aerobee 150A, an $8^\circ \times 8^\circ$ field is scanned in 1 sec of time, or at 64 deg^2/sec.

The stray-light environment of the above application typifies that encountered by most fully gimbaled systems. The FOV is required to work as close as possible to the Sun or the sunlit Earth's limb to maximize the availability of guide stars at all times regardless of season or position of the vehicle in orbit. The stray-light environment, the acquisition time, and the tracking-accuracy performance asked of these trackers (without the benefit of platform stabilization to extend time constants) constitute one of the more formidable sets of operational requirements to be met by state-of-the-art equipment.

Useful experience was gained from the OAO tracker program.

Tests during design proved that use of an astrodome for total enclosure of the tracker was infeasible for this application because of noise introduced by impinging sunlight. The resulting open design required special attention to choice of materials and to space lubrication of moving parts (bearings and brushes) in vacuum.

A stray-light shield was successfully developed, which had a one-stage attenuation for earthshine up to 14° and a two-stage attenuation of 10^{12} for sunlight up to 30° from the optical axis.

The phototube required special selection and treatment for star-tracker duty. Spectral response and tube orientation to the optical center line were found critical to threshold sensitivity. Special shielding was required to eliminate pickup.

The first flight was aborted after 21 Earth orbits following a succession of problems terminated by battery failure. Postflight analysis and test suggested the possibility of tracker high-voltage corona as a contributing factor along with failure of battery sequencer. Lack of positive venting at high voltage supply allowed the possibility of partial-pressure conditions conducive to corona from turn-on at 55 min after launch to 21st orbit. Modifications were subsequently made on tube shielding and voltage supply to obviate corona at all pressures.

2.7 Fine-Guidance Trackers

The most demanding accuracies for attitude control have been associated with spacecraft carrying large optical-experiment packages. For fine guidance of such experiments, a star tracker can be located either within or adjacent to the experiment optics with its optical axis boresighted to the experiment. The pointing accuracy in this type of application is expressed in terms of the experiment line of sight (LOS) relative to its target.

When integrated with the experiment optics, the fine-guidance tracker can be designed with an effective focal length and aperture much larger than is normally possible within the size and weight limitations of a separate tracker. The integrated form can thus provide greater accuracy and can track on fainter targets.

A number of balloon-borne experiments having fine-guidance trackers have been sent aloft to perform spectrometric and polarimetric measurements on planets from altitudes of 70 000 to 120 000 ft. Though not spaceborne in the fullest sense, such tracking equipment deserves mention because it demonstrates state-of-the-art capability from 1959 to 1968 for fine guidance under circumstances close to the spaceborne applications that are now coming to fruition.

Notable for its angular sensitivity is Stratoscope II (refs. 7 and 17), in which the 36-in. aperture of an infrared (IR) experiment is followed by optical relays so as to obtain an F/50, 150-ft effective focal length image for use in 0.01 arcsec tracking. On the first ascent the system tracked the Moon, Jupiter, and eight stars. On later flights, a 0.02-arcsec pointing accuracy was demonstrated. Some difficulty was encountered with the acquisition of Mars in a small FOV because of the relative angular velocity imparted by balloon rotation.

The susceptibility of star trackers using electron-ballistic detectors to high-voltage corona was encountered by the trackers for the Stratolab High and Polariscope balloon systems. Fortunately, the phenomenon was first noticed in ground tests that duplicated the partial-pressure environment conducive to the phenomenon, and it was rectified before flight.

Recent examples of integrated fine-guidance star trackers for spaceborne optical payloads are to be found in the Princeton Experiment Package (PEP) and the Goddard Experiment Package (GEP) (ref. 18), both of which were developed for the OAO. Each experiment was pointed by the spacecraft so as to keep the ultraviolet (UV) energy of the target centered within the entrance slit of a grating spectrometer. The fine-guidance system for the PEP derives its signal from star energy collected by the 80-cm aperture of the experiment and reflected off the jaws of the spectrometer entrance slit. In the GEP, the fine-guidance tracker is fed 9 percent of the star energy collected by the 96-cm aperture of the experiment telescope. The tracker focuses this energy with its own Dall-Kirkham telescope onto tuning-fork modulators and to a photomultiplier.

The OAO vehicle also carries a boresighted star tracker, which is separately mounted on the spacecraft near the entrance aperture of the experiment. This unit employs an image dissector and tracks either the experiment target or a nearby guide star. The latter offset mode allows the experiment to be trained on nebular targets. The boresighted star tracker has successfully functioned on the A2 flight.

2.8 Summary

Much valuable experience in spaceborne star-tracker design has been accumulated within the past 8 years. On almost every program the outstanding problem of stray light was encountered in one or more of its various manifestations. The sources are now well understood, but in each new design the stray-light propagation within the tracker and its effect on the signal channel must be examined.

A second major problem has been the phenomenon of corona associated with the use of electron-ballistics detectors. Solutions have been found to this problem and to the many lesser difficulties that accompanied the first designs of each type of tracker.

Some difficulties that were expected never became significant (ref. 12, pp. 2-100). In this category are the phenomena of micrometeoroid erosion and radiation damage. Precautions must still be taken, however, when the mission duration or flightpath is such as to maximize these hazards (ref. 19).

Through optimal design techniques and the careful selection of components, tracking systems can now be designed to be lightweight, rugged, and reliable, and to maximize the inherent photon efficiency of the detector. Perhaps the most important lesson to be learned from the equipment flown to date is the recognition and understanding of the total design problem, from noise to thermal stability, before irrevocable design decisions are made.

3. CRITERIA

Star trackers shall be designed to acquire and provide tracking signals relative to specified stars under all anticipated flight conditions. The design shall achieve specified accuracy and reliability of performance within allotted space, weight, and power-consumption constraints. The design shall minimize susceptibility to error sources inherent in the operational environment and the vehicle installation. Compatibility with tracking control accuracy and dynamic performance requirements shall be assured.

3.1 Input Phenomena

3.1.1 Stars to be Tracked

A precise specification of the stars to be tracked shall be established that takes into account

(1) Availability in the preferred region of the sky
(2) Freedom from confusion with neighboring stars
(3) Adequate brightness
(4) Spectral characteristics

3.1.2 Star Signal

The estimated star signal developed by the tracker from specified stars should take into account

(1) The spectral sensitivity of the optical system and the detector
(2) The spectral distribution of the star energy
(3) The effects of modulation or scan efficiency

Estimated star signal values should be verified by test wherever marginal conditions exist.

3.1.3 Random Noise

It should be assured that random-noise sources inherent in the incident light and from internal sources do not degrade the probability of successful star acquisition. As a minimum, the following noise sources shall be considered in analysis and tests.

(1) Background light
(2) Stray or extraneous light
(3) Photodetector noise
(4) Illuminated particles in FOV
(5) Thermal noise circuitry immediate to photodetector output

3.1.4 False Signals

It should be assured by analytical procedures and tests under simulated conditions that false signals generated by background or stray light do not degrade star-tracker performance. Background and stray-light sources to be considered include

(1) Celestial bodies in or near sky region containing specified stars
(2) Particulate debris that may be shed by the spacecraft
(3) Internal reflections
(4) Spacecraft elements in FOV

3.1.5 Interference Sources

It should be assured that sources of noise other than thermal and shot noise are held to a minimum. Sources to be considered include

(1) Microphonics
(2) Radiofrequency interference
(3) Audiofrequency pickup
(4) Electrostatic-charge leakage
(5) Low-frequency-impulse noise

Microphonics should be evaluated by tests of the tracker under expected vibration conditions.

3.2 Performance

3.2.1 Acquisition

The acquisition-mode design should provide combinations of search area and search time such that the resulting search rate and the star signal threshold logic will insure the required probability of recognizing the desired star and rejecting unwanted star images. The following factors should be taken into consideration in the design of the acquisition mode:

(1) Search-area size and shape
(2) Vehicle drift during search time
(3) Signal and noise levels during acquisition
(4) Optical efficiency
(5) Photodetector response, both photometric and dynamic
(6) Electronic gain, threshold values, and logic
(7) Calibration uncertainties
(8) Optical interferences
(9) Changes in above parameters due to aging, drift, vehicle orientation, etc.

3.2.2 Tracking

It should be assured by analysis and tests that the performance of the tracking subsystem is adequate for the continuous tracking of selected stars within mission requirements. Factors to be taken into account include

(1) Motion of tracker mounting base
(2) Extraneous light in FOV and other noise sources
(3) Accuracy requirements
(4) Minimum star signal
(5) Tracking bandwidth

(6) Random error from system noise
(7) False signals

3.2.3 Index Error

All potential sources of index shift should be identified during design, and the root sum square contribution should be held below allowable index error. Potential sources of index error to be considered in the analysis include

(1) Structural stability between scan or modulation system, the optical system, and the mounting reference points or pads
(2) Mechanical shock and vibration during thrusting flight
(3) Thermal effects

3.3 Design Considerations

3.3.1 Photodetector

The photodetector shall satisfy both mission requirements and design constraints. Control of characteristics that influence system performance should be assured by specifications, selection criteria, and individual component tests oriented to the specific type of detector involved.

3.3.1.1 Photomultipliers

The following factors should be given special consideration when photomultiplier tubes are used:

(1) Ruggedness and microphonics
(2) Spectral response range and responsivity
(3) Nonuniformity of detector response
(4) Tolerance on photocathode location within tube
(5) Temperature effect on dark-current noise and spectral response (Design temperatures should never exceed 75° C.)
(6) Need for suppression of corona discharge
(7) Fatigue of photocathode at high levels of irradiance
(8) Shielding of tube from electrostatic and magnetic pickup and strong stray fields that can alter tube gain
(9) Dynamic response limitations imposed by associated circuitry
(10) Shielding from radiation environment

3.3.1.2 Image Dissectors

The following factors should be given special consideration when using image-dissector tubes:

(1) All items discussed in section 3.3.1.1 for photomultipliers
(2) Nonuniformities in cathode sensitivity, especially near or at the central region of photocathode
(3) Sensitivity to weak magnetic fields that can contribute index error
(4) Curvature of photocathode surface with respect to the focal plane of the optics
(5) Need for shake test to verify electrode stability at front of image section

3.3.1.3 Vidicons

The following factors should be given special consideration when using vidicon tubes:

(1) Ruggedness and microphonics
(2) Signal current versus illumination characteristics
(3) Resolution (effective beam size)
(4) Coherent noise (hot spots) including development of additional hot spots with time and temperature
(5) Optimum raster line spacing for image and beam sizes
(6) Limitation on angular tracking rate resulting from finite target-integration time
(7) Need for suppression of corona discharge
(8) Faceplate temperature and dark current
(9) Shielding of tube
(10) Persistence of image on photoconductive cathode
(11) Filament susceptibility to shock

3.3.1.4 Solid-State Detectors

The following factors should be given special consideration when using solid-state photodetectors:

(1) Preamplifier noise figure
(2) Pickup from modulator power line
(3) Working temperature
(4) Firmness of connecting leads
(5) Environmental stability requirements

Specifications for a silicon photodiode detector should include

(1) Leakage current (affects internal noise)
(2) Responsivity (amps/W)
(3) Resistivity (ohms/cm)
(4) Junction depth (determines spectral response)
(5) Uniformity of responsivity over usable area

Specifications for a CdSe detector should include

(1) Conductance versus irradiance over spectral range of interest
(2) Cell noise versus background irradiance
(3) Time constant for given cell current
(4) Background illumination effects on time constant
(5) Uniformity of conduction over usable area

3.3.2 Optics

3.3.2.1 Image Formation

The optical system should be designed to provide a circle of confusion over the entire working field of view consistent with the minimum detectable error. A lightweight, rigid assembly of elements having as few surfaces and as high transmission as possible should be specified that has minimum sensitivity to thermal effects.

Where refractive elements are used, care should be taken to pass all the spectral power seen by the sensor, and chromatic aberration should be controlled over the spectral range of the detector and field of view.

Aperture should be adequate to assure adequate working values of $S/\tilde{N}$ for acquisition and for random tracking accuracy with due allowance for vignetting.

Optical efficiency should be kept above 50 percent if possible.

The deposition of lubricating oils or greases upon nearby optical surfaces should be prevented.

3.3.2.2 Shielding

The design of a shield should attenuate stray light from sources outside the FOV. The geometry of shielding specific to each source should be separately considered. The analysis of stray-light propagation toward and within the tracker optics should consider the finite reflectance of black paint, the surface scattering of clean optical surfaces, and the internal reflections and volume scattering possible within refractive optical elements.

A shutter must be provided where exposure of the star tracker to direct sunlight or to other sources of excessive light that can damage the photodetector is possible. The shutter mechanism used must be of very high reliability because of the catastrophic effect of its failure.

3.3.3 Mechanical Design

3.3.3.1 Structure and Materials

Design of the star-tracker structure must satisfy index-error stability requirements. Lightweight structural materials that are dimensionally and chemically stable in the space environment should be chosen. Surface coatings and other substances near optical elements must not powder or shred.

3.3.3.2 Thermal Considerations

Thermal analysis of the star tracker must be initiated early in the design and repeated for each significant change in requirements. The tracker thermal design must include a spacecraft system analysis that considers the thermal interchange among spacecraft, tracker, and space environment.

3.3.3.3 Lubrication

For mechanical parts, such as bearings, brushes, and solenoids, that are exposed to pressure levels under 10^{-6} torr, acceptable materials and lubricant should be used to avoid space welding.

3.3.4 Electronics Design

3.3.4.1 Circuitry

Star-tracker circuitry must be designed to amplify weak signals from the photodetector without introducing interference. Circuitry must not deteriorate the basic S/N ratio present at the detector output.

3.3.4.2 Corona Suppression

Preventive measures against the occurrence of corona discharge at all specified ranges of temperature and pressure should be incorporated at the design stage. Any electrical potentials above approximately 100 V should be suspected. Dependence upon the low pressure of orbit is not an adequate safeguard because of the contingency of accidental turnon before reaching orbit or before outgassing is complete.

3.4 Alinement, Calibration, and Test

3.4.1 Internal Alinement

Provision should be made during design for a final determination or setting of the star-tracker LOS with respect to the tracking-unit outer surfaces that interface with the space-vehicle reference framework. Internal angular alinement shift during subsequent test should not exceed the allowable index error.

3.4.2 Calibration

Calibration of the star-tracker sensitivity with respect to star recognition thresholds and tracking sensitivity must be performed using a well-collimated star simulator of known intensity and spectral distribution, and include tests of the star-tracker response over the entire field of view. It should also include procedures to determine the spectral response of the device and the effects of various star "colors" on photometric calibration.

3.4.3 Test with Spacecraft

Means for insuring proper boresight alinement of the star tracker when mounted on the spacecraft must be provided.

A simulated star source should be provided for on-pad checkout of alinement and sensitivity of the mounted star tracker. Tests of at least "go" or "no-go" quality will be necessary.

4. RECOMMENDED PRACTICES

4.1 Input Phenomena

4.1.1 Stars

4.1.1.1 Star Availability

Availability must be assured by examining the mission profile for the relative positions of bodies, such as the Earth, Sun, Moon, or spacecraft, that may obscure the candidate stars or cast intolerable levels of stray light into the tracker. The area of search for star acquisition must be sized and directed so as to assure the inclusion of any specified star and the exclusion of any other stars or bodies that the system is unable to discriminate against by magnitude, color, or position.

Known astronomical data should be converted into terms that indicate actual star signal levels and availability for the specified stars that best serve the system requirements. For example, at least one trackable star may be needed with 100 percent probability in a direction normal to the ecliptic plane as seen from a specified location on the spacecraft during the midcourse phase of a translunar trajectory, regardless of the time of year. The factors influencing selection are shown in a flow relationship by figure 2.

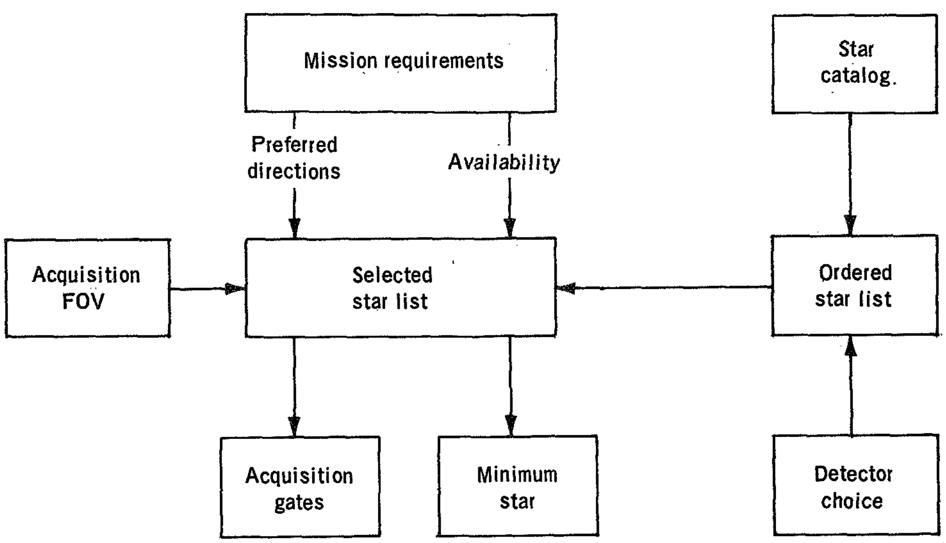

Figure 2.–Star selection.

When many stars must be detected and tracked, they should be identified and ranked in accordance with their effective photoelectric strength. The spectral data used for this purpose should be precise. For example, the approximations involved in the use of star blackbody curves or published detector spectral response may introduce errors in stellar signal (typically 0.3 mag) from either approximation. Total errors of 0.5 mag will occasionally be encountered on some star/detector combinations.

In the determination of effective star signal from the star photocurrent, consideration must be given to modulation or scan efficiency. If the modulation efficiency assumes a well-resolved star image near the diffraction limit, the actual star image must at least be verified by measure. This measure should include the energy within the spectral range of detection. In any case, the combination of optics, modulator, and detector must be subjected to test.

Star catalogs are available that list stars by names, direction, color, and star magnitude or relative brightness (refs. 20 and 21). In general, however, the selection of a group of stars with absolute locations satisfactory to the mission and relative spacings sufficient to avoid ambiguous acquisition requires a more precise knowledge of their ranking in terms of effective irradiance.

4.1.1.2 Star Signal

Weight the power spectral distribution of each star by the relative spectral response of the chosen sensor to determine the effectiveness of star energy in producing photodetector output. Some methods for implementing this step are described in the following paragraphs.

Star magnitudes are converted from the usual photovisual to a photoelectric basis. The result is a listing, where the detector, rather than the eye, shapes the spectral window through which the star energy is seen. Often the conversion term is listed as an additive correction to visual magnitude and is referred to as the color index. The photoelectric magnitude scale is indexed with respect to the visual scale so that the two have like values for stars of the particular spectral class. Star magnitudes assigned by this method are sometimes identified by the detector characteristics; e.g., "S-20 magnitude."

Bolometric magnitude rating and the effective color temperature may be used. Bolometric magnitudes are independent of star color and may be determined by applying a bolometric correction to the photovisual magnitude. The reference standard for zero-magnitude bolometric irradiance is 2.27×10^{-12} W/cm^2. Details of this method may be found in reference 22.

The use of star response tables prepared by the Lunar and Planetary Laboratory (LPL) of the University of Arizona is a third method. This group has prepared tables that identify the 985 brightest stars north of declination $-20°$ by number, color, location, and visual magnitude. For each star, the response from seven representative star detectors is given in amperes per square centimeter of effective aperture. These tables are recommended as the most direct and accurate means for predicting star currents. They were generated in response to NASA's desire for a new star list that would supersede all previous data (including the Smithsonian tables) and that would be unhampered by the classification of stars according to color temperature or spectral type.

A condensed version of the LPL data for 57 navigational stars is provided in Appendix B. Included are the spectral sensitivity curves used in computing the current response of seven detectors. Six of these represent the most used photocathode materials for photomultipliers and image dissectors. The seventh is typical of the red-sensitive silicon photodiode. The ratios of amperes to watts given by the curves are typical of such detectors when they are operating as current sources into a negligible load impedance. Total star current is obtained by applying the appropriate factors for total aperture, optical efficiency, and optical transmission over the spectral range of detector sensitivity.

With the stars sorted according to their effect on a chosen detector, a set of available stars can be chosen that yields no ambiguities for the specified area of search. This selection is best made by computer. The search area should be just large enough to accommodate the initial pointing error of the tracker as determined by the spacecraft system. The weakest star, as revealed by the final unambiguous list of selected guide or target stars, is then used as the basis for determining the key design parameters affecting tracker performance.

Because of their importance in the application to a given star list, the differences in spectral response found in different samples of the same type of detector bear watching. The spectral response can vary significantly with temperature for a photoemissive surface and with depth of dopant for a silicon detector.

4.1.2 Random Noise

Sources and system points of entry for random noise are indicated in figure 3. Formulas recommended for determining the combined effect of noise sources are given in Appendix C for each major sensor type.

In space, the noise contribution of background light seen within the FOV is negligible if the mission is based on the relatively bright navigational stars. Faint star targets (e.g., +4 mag or weaker) may require the estimation of light from neighboring weak stars and possibly of the zodiacal light that appears in the instantaneous FOV.

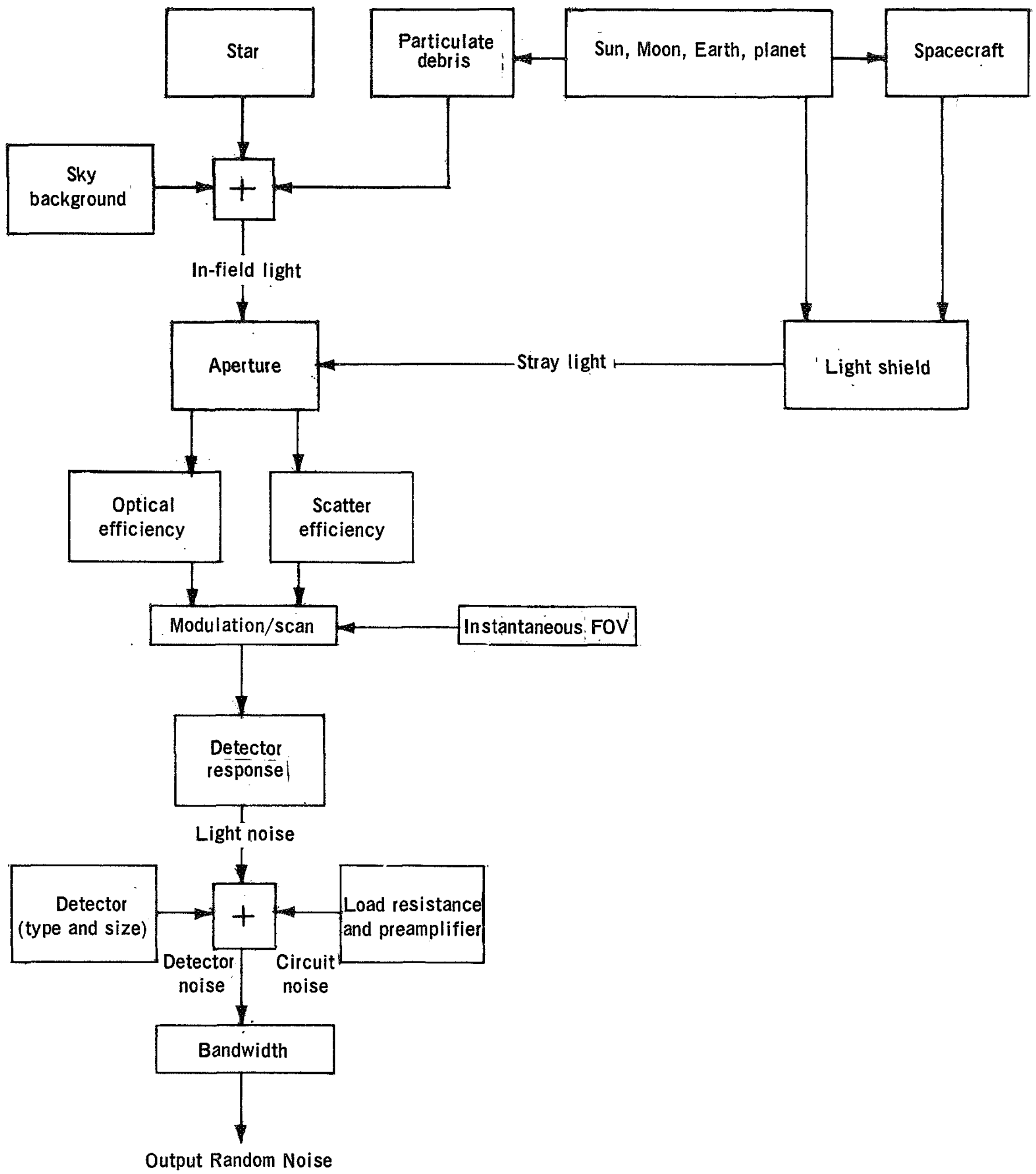

Figure 3.—Sources of random noise.

Estimate the background contribution of scattered sunlight if tracking is required when the vehicle is within the geosphere up to at least 50 km altitude (27 n. mi.). Airglow and aurora can be factors from 40 to 100 n. mi., and for star observations near the Earth's horizon, can appear from 100 to 1000 n. mi. orbits as in-field background light (ref. 20).

An additional source of in-field light known to cause significant levels of noise is the presence of particulate debris associated with the spacecraft and illuminated by the Sun.

Light scattered into the optics by the Sun, Earth, Moon, the spacecraft, or its particulate debris constitutes the greatest uncertainty in the prediction of noise.[2] This uncertainty can best be reduced by

(1) Identification of all situations whose geometry is conducive to the interception of scattered light
(2) Creation of a physical model simulating the source, scattering surfaces, and star tracker[3]
(3) Measurement of noise currents for various attitude changes in model geometry

4.1.3 False Signal

The tendency of a star-tracking system to generate a false or apparent star signal can be minimized by good design practice. However, the actual level of false signal is difficult to estimate and is best determined by test. As in the case of noise, the primary effects stem from extraneous light inputs. The factors involved are shown in figure 4. Unfortunately, the system techniques used to enhance signal in noise will enhance false signal as well.

4.1.3.1 Nonuniform Illumination

Light from nonuniformities in the background, such as star groups (ref. 23), the faint glows of the Earth's limb, nearby sunlit particles, etc., can be readily modulated into false signals. A large instantaneous FOV is particularly vulnerable. The recommended procedure for minimizing the effect of background gradient is to make the instantaneous FOV small and the spatial modulation comparable to the diameter of the star image. With mechanical modu-

[2]Because the Sun is of the order of 10^{12} times as bright as stars being tracked, the magnitude of the light being scattered into the optical system can be considerable. For example, sunlight impinging at 30° off the axis of a lens will cause an apparent brightness of approximately 140 ft-L (22.4 W/m^2) for every 1 percent of scattering.

[3]For best results, the source should be full scale in terms of angular dimensions and intensity, while all receiving surfaces should be physically in full scale. Unrepresentative scatterers, such as dust and air molecules (if significant), should be removed by evacuation of the test chamber to at least 10^{-5} torr.

lators, the FOV is usually subdivided into small sections having dimensions comparable to star size. With image dissectors, the scanning aperture can be made small, and with vidicons, the scanning-beam diameter is made comparable to the star image.

The same measures serve to minimize the false signal generated by stray light scattered from extra-field sources, causing them to fall nonuniformly at the focal plane.

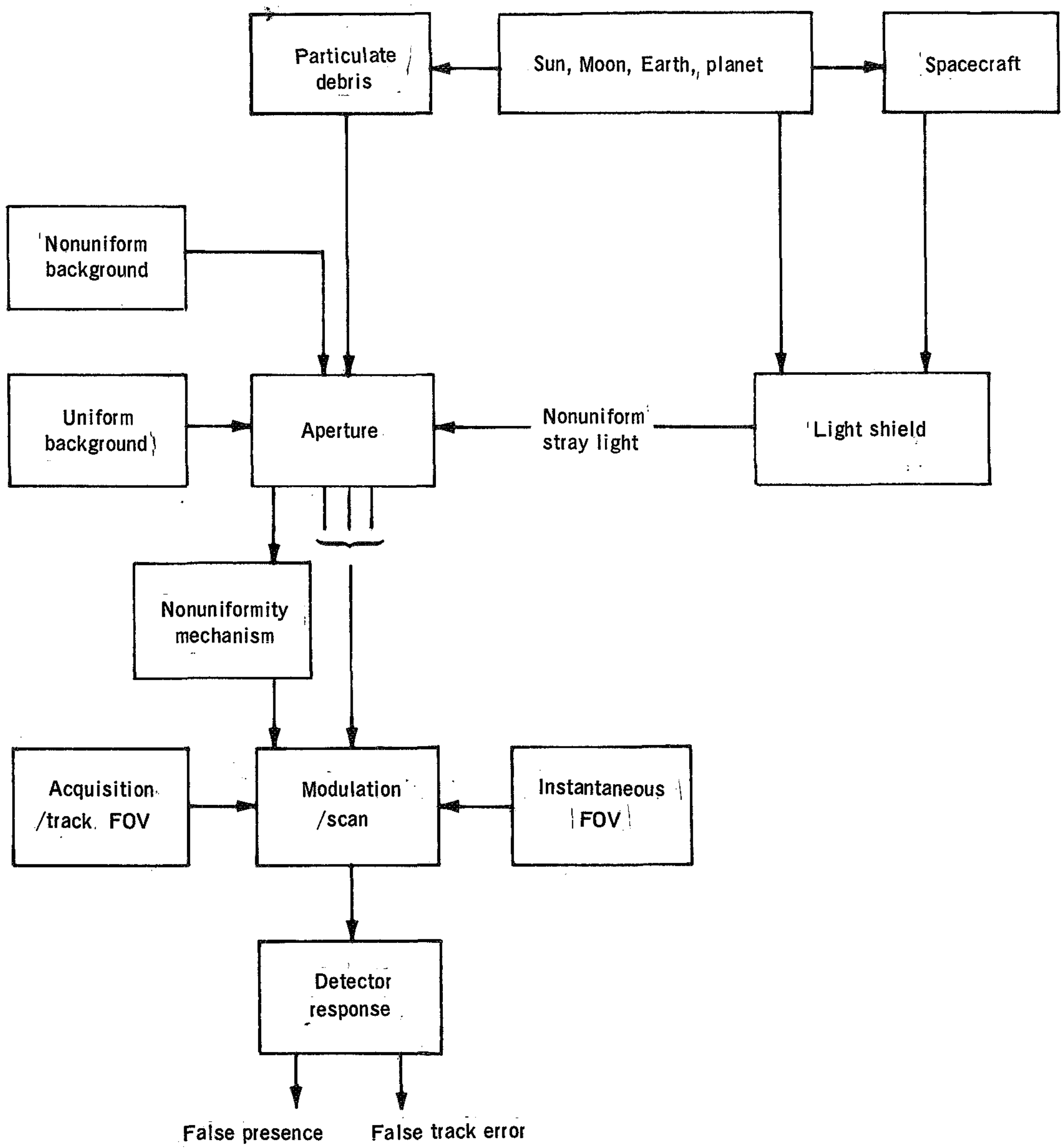

Figure 4.—False-signal generation.

4.1.3.2 Uniform Illumination

The process by which a uniform background can develop a false star signal is more subtle, and is usually based on some asymmetry in the optics or nonuniformity in the photosensor.

For example, a mechanical scan that moves a pattern of alternately opaque and transmitting slots across the acquisition FOV as defined by a fixed field stop will easily chop uniform illumination at the focal plane. Theoretically, the false signal may be minimized by designing the slots to a precise ratio with the field stop. A less vulnerable mechanical scan may be devised by using only a relative motion between the star image and field stop, such as that offered by rotating wedges or by carrying the stop on a vibrating reed or fork.

Electronic scan systems can effectively suppress false-signal generation in a uniform background because the small instantaneous field can be easily swept throughout the acquisition field.

Small hot spots in a vidicon or spatial variations in the cathode sensitivity of an image dissector can generate false signal during the electronic sweep. Even a photomultiplier, which is usually located beyond the focal plane, at a point where the entrance pupil is imaged, can develop false signals because of the variation in the angle of incident light as the modulator scans the focal plane.

4.1.3.3 Particles

Sunlit particles in the near field of the optics may appear in sufficient focus for false-signal generation if they are at distances that are large compared to the focal length (e.g., 10×). As such particles come closer, they cast more light into the optics, partially offsetting the effect of defocus. Design measures available for minimizing the influence of such particles include

(1) Use of modulation or scan system sensitive only to small images
(2) Incorporation of maximum and minimum threshold gates for star acquisition
(3) System rejection of sources having angular velocity in inertial space
(4) System rejection of sources that lie outside the expected star direction

4.1.4 Miscellaneous Interference

Other noiselike sources of interference can significantly affect acquisition and tracking if not sufficiently controlled. These sources are sometimes regular or coherent in nature and are usually confined to one or more frequency bands. Interference components at signal frequency are interpreted as false signals.

4.1.4.1 Microphonics

Microphonics readily develop when detectors are housed in vacuum tube envelopes (1P21, image dissector, vidicon) and in the signal leads from low-output-level detectors (solid-state and vidicon types). Because the detector must be rigidly related to the optics and the structure of the housing and because tracker housings must usually be rigid with respect to a mount or reference structure, vibration isolation is not normally recommended. The best way to prevent microphonics for vacuum tube types is to use rugged construction.

4.1.4.2 Radiofrequency Interference

Radiofrequency and audio pickup require the usual precautions.

4.1.4.3 Electrostatic-Charge Leakage

Leakage of electrostatic charge, frequently manifested as corona, introduces impulse noise into the tracker circuitry, and under some conditions, directly into the photocurrent, by creating light flashes visible to the detector. Protective measures are discussed in section 4.12. (See also ref. 24.)

4.2 Performance

4.2.1 Acquisition

4.2.1.1 Search Program

The best method for covering the required search area is dictated by the size of the area, the form of star tracker, and the choice of modulation or scan. The search plan should take into account motions inherent in the modulator or scan system, shape of the search field, the region of maximum star probability, and any pointing drift.

In some applications, such as the Canopus trackers on Surveyor, Mariner, and Lunar Orbiter, a spacecraft roll rate was used to move the acquisition field through the search area. In this case, complete search is assured simply by maintaining the proper roll rate and axis.

Excessive attitude drift of the spacecraft during search can lead to skipping areas in the pattern. If angular drift information can be made available from an onboard inertial reference, the search pattern can be compensated. Otherwise, only an increase in search rate can prevent the occasional occurrence of holes in the pattern.

The search rate resulting from the choice of operational parameters influences the noise level present during star acquisition. For photoemissive detectors operating with a specified signal level on an essentially dark background, the required rate may be accommodated simply by increasing the instantaneous FOV. Improvement in this direction is limited by the fact that the background noise will not remain insignificant as more field is seen by the detector. Also, the system becomes more vulnerable to false-signal generation and stray light.

For the majority of applications, the size of the instantaneous FOV has little effect on the maximum allowable search rate if a given working S/N ratio is to be maintained.[4] It is therefore recommended that the instantaneous FOV be kept small.

4.2.1.2 Acquisition Probability

In an optimum design for acquisition performance, the controllable sources of random noise, false signal, and other forms of interference should be held to negligible levels compared to the random noise generated by the irreducible background, stray light, and internal quantum-mechanical energy exchanges of the detector system. This condition can be tested by evaluating the influence of each identifiable source upon acquisition probability. Some, like false signal and rectified pickup, alter the true value of minimum star signal. Others, such as microphonics and excessive preamplifier noise, may combine with irreducible random noise. See figure 5 for factors of acquisition.

The influence of random noise upon star acquisition imposes the finite probability that a desired star may be missed (P_1) and that noise itself will initiate a false recognition (P_2). The resulting probability of correct acquisition $P_c = 1-(P_1 + P_2)$ depends on how the

[4]This rule can be shown to apply either where background noise is dominant or where solid-state sensors are used, or both. In such cases, noise power increases directly with instantaneous FOV. To maintain S/N this FOV must be swept more slowly, leaving the same search area to be covered in the same search time. The same rule applies to vidicons for different reasons.

program of search and acquisition is engineered against the available S/N ratio. A gaussian noise distribution can be assumed for determining these probabilities. (See ref. 25.)

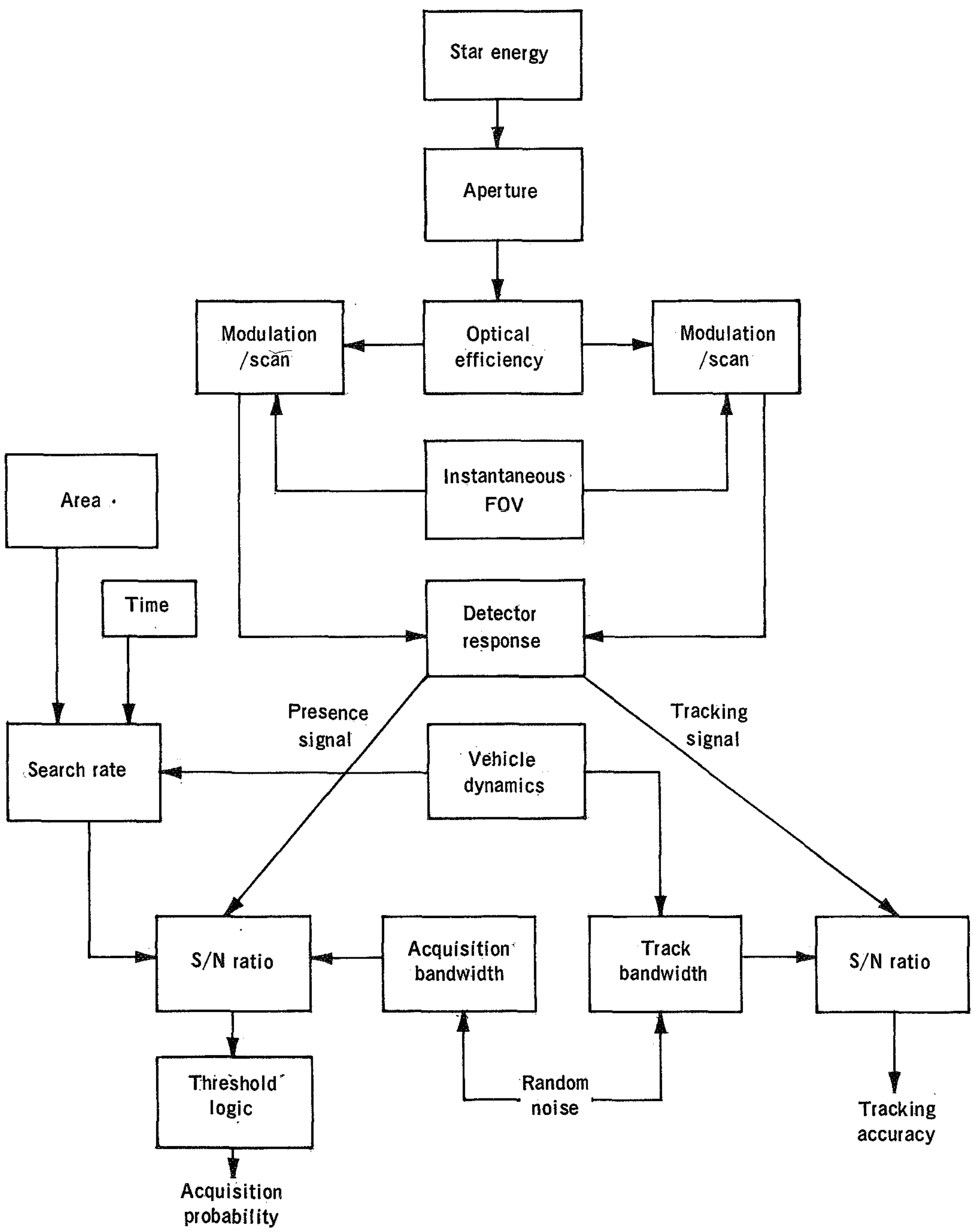

Figure 5.–Factors of acquisition and tracking.

During a typical acquisition, the star signal appears (or is modulated) for a brief period, rising as a function of bandwidth past the detection threshold to a maximum level S, in the presence of rms noise N. Acquisition logic indicates star presence whenever the value of N or S+N passes the threshold.

As a rough rule, a peak-signal to rms-noise ratio of 6:1 should be provided during acquisition if a 99-percent probability of correct acquisition, P_c, is to be maintained. If the specified P_c cannot be met, either changes in basic design parameters can be instituted or the operational parameters must be revised to increase signal or decrease noise current.

Some improvement in P_c can be achieved by variations during the search program. Regions of search known to have a lesser chance of containing the star may be scanned faster. Two stages of search may be used, the first being a full scan with higher bandwidth (and higher P_2) over the whole field, and the second a verifying scan (with low P_1 and P_2) limited to those areas reporting signal in the first scan.

The obvious step of increasing aperture so as to boost signal level usually increases equipment weight and volume proportionate to the cube of the aperture. Because of this steep tradeoff, the initial spacecraft system criteria for star availability and for the search rate required on the minimum star deserve special scrutiny.

4.2.1.3 Threshold Logic

The use of a threshold also serves to minimize acquisition of the unwanted weaker stars. In some applications where unwanted stars exist that are brighter than the selected group, a second threshold is useful as a maximum gate. Acceptance criteria may be further augmented by the requirement that the signal to be recognized persist, or repeat, in a way characteristic of a steady star. This logic assists the rejection of moving particles, stray-light glint, and impulse noise that may be generated at the detector.

The optical transmission, photodetector sensitivity, and system forward gain may vary over a protracted mission so that the star presence signal can change its calibration by as much as 0.5 mag. Where precise discrimination is required, means of readjustment is recommended. For example, if near-neighbor stars are to be identified in a field of weak stars, calibration may be made on a reference star. Gain or threshold may be re-adjusted by onboard programing or by ground command.

4.2.2 Tracking

Design factors involved in the determination of tracking performance are shown in figure 5.

4.2.2.1 Tracking in Noise

Random tracking error should be controlled by maximizing the ratio of signal change per unit error angle to random-noise level as seen at the system output.[5] This incremental S/N ratio is improved by

(1) Reduction of noise sources
(2) Reduction of tracking bandwidth
(3) Increase in the percent of total star energy that is converted to signal for a given change in error angle
(4) Increase in the total collected star energy

The minimum level of system noise should be achieved by application of the recommendations in sections 4.1.2 and 4.1.4. The contribution of photodetector noise usually increases with temperature, requiring confirmation of temperature range expected in the operating environment.

The lower limit of bandwidth is set by the dynamic response required of the nulling servo to cancel the effects of vehicle motion. Such motion is typified by the operation of the attitude-control system through a dead band; e.g., coasting at 0.1°/sec through a ±1° band.

In designing against vehicle dynamics, a distinction should be made between the level of motion (angular acceleration and velocity) to be accommodated with full tracking accuracy and the motion to be tolerated without losing the star from the FOV.

To maximize the part of star energy converted to signal by a unit change in error angle, the angular diameter of the star image should be brought to a minimum. A modulation technique should then be chosen that is sensitive to changes in star direction. This practice concurrently reduces the angle-from-null at which the star signal reaches a maximum. At this point, signal proportionality stops, and the signal either remains flat or droops as the edge of the tracking FOV is approached. The resulting nonlinearity can affect the stability and hence the available performance of the servo system used to drive the star image to null.

Star energy per error angle is also increased by design practices that increase the total received star energy, such as optical aperture and transmission.[6]

In summary, the vehicle dynamics ultimately limit the S/N that determines random tracking accuracy. If the latter fails to meet requirements, basic changes in design parameters must be

---

[5] In a system offering a proportional error signal in the region of tracking null, this ratio equals 1 at the noise equivalent angle.

[6] Although these same steps increase light noise, a net increase in S/N is achieved. In most systems, the increase comes as the square root of the increase in collected star energy.

instituted, such as an increase in aperture. Such steps usually involve a steep tradeoff against weight and volume. The initial spacecraft criteria for allowable uncompensated vehicle motion therefore deserve special scrutiny.

4.2.2.2 Tracking with False Signal

False signal biases the tracking signal so that an equal and opposite star error signal is present at null. The results are a bias error in tracking and an unbalance in the maximum signal levels at the ends of the error characteristic. In the presence of noise, the latter effect can lead to noise rectification and the generation of additional star-tracker pointing error.

The amount of bias error is not governed either by signal versus error slope or by bandwidth. It can be controlled to some extent by a reduction of tracking FOV. Rectification error is minimal if the error characteristic does not saturate until well beyond the noise equivalent angle (NEA); for example, at five times the NEA.

4.2.2.3 Gain Control

Constant tracking-system gain is usually provided by controlling the tracking gain in inverse proportion to star-presence measure in a fashion similar to radio-receiver gain when controlled by carrier level (AGC). For tracking systems that must accommodate a wide range of star levels, it is recommended that the feedback point for AGC insertion be located at or as close as possible to the detector to minimize the problem of signal and noise saturation in subsequent circuitry.

In detectors having photomultiplier action to amplify the photocurrent, the dynode voltage supply can be used for AGC feedback. Such a system has been successfully employed using the high exponential gain of dynode voltage to accommodate star differences of 5 mag (100x) with an output variation of only 15 percent.

4.2.2.4 Tracking Mode for Scan Systems

For the vidicon, tracking error signals are derived from the timing of the star pulse within the scan-beam-deflection program. The beam scan generally does not register exactly over the star image, resulting in both a weakening of star pulse and multiple pulses on one star. To improve the tracking performance of a vidicon, the following is recommended (ref. 26):

(1) Confine the scan signal by electronic blanking to region of interest, once a star is located. If scan is to be localized, consider the danger of photosensitive-surface damage.

(2) Select optimum scan line spacing for given image and beam size.
(3) Average the positions of repeated scans.

4.2.3 Index Error

Special attention must be given to the dimensional integrity among optics, modulator/detector, and housing. Within the modulator/detector, both mechanical and electronic stabilities need scrutiny. To identify the variables in exploratory test, separate vibration, thermal, electronic-overload, and other tests should be performed. Acceptance tests should not include the threat of incipient component destruction. The factors of index error are shown in simplified relationship by figure 6.

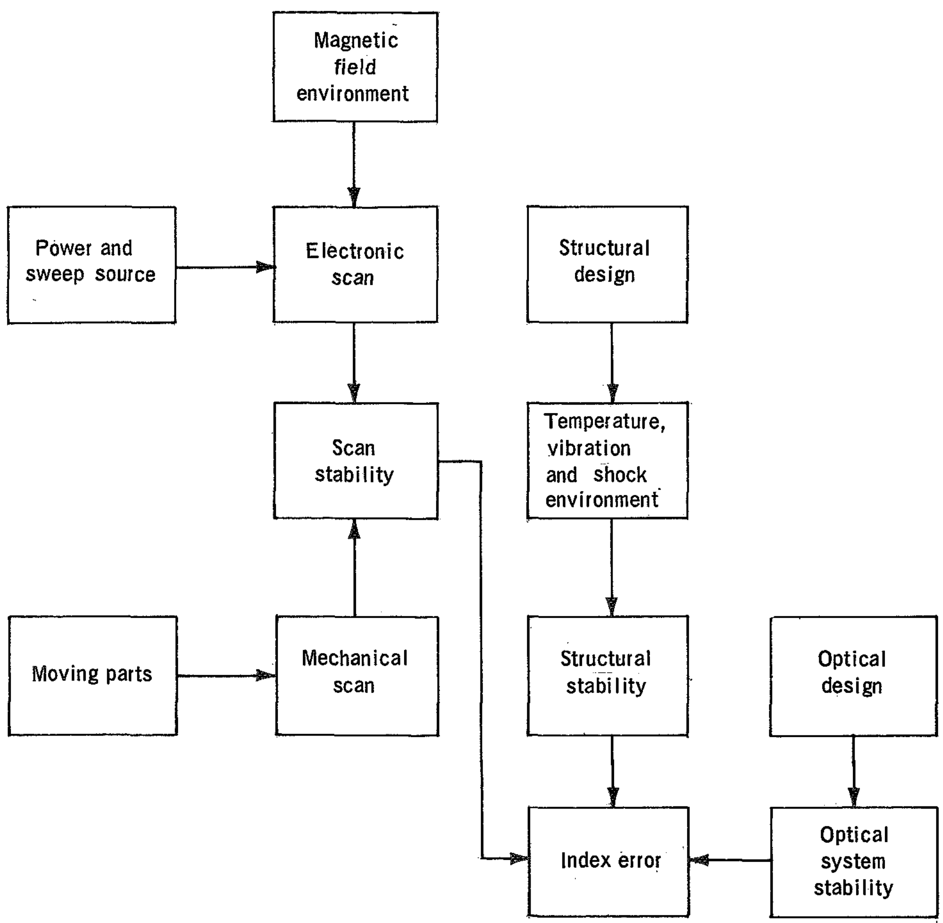

Figure 6.—Factors of index error.

It is common practice to specify index error to the same range as the sum of allowable random errors. If this sum is in the arcsecond range (e.g., 5 arcsec) the evaluation of index accuracy can be elusive. The various environmental factors (shock, temperature, etc.) can appear in critical combination during storage, transportation, test, and flight; and the influence of aging on dimensional stability is an indeterminate function of such factors. The equipment that measures index error should be 5 to 10 times more accurate than is the device under evaluation.

If small index-error specifications are to be guaranteed, size and weight of the tracker will increase. Fortunately, spaceborne missions have access to known stars as perfect collimators spaced at known angles, making a redetermination of any index error possible. If operational procedures can be arranged to exploit this possibility, a significant reduction in star-sensor weight and cost can be effected.

4.2.3.1 Mechanical Modulation Stability

In a mechanical scan/modulation system, the center of scan is typically the center of rotation of a shutter bearing or the point of midswing for vibrating reeds or tuning forks. The effect of wear must be considered for the rotating system, and the stability of the mounting and electronic drive for the vibrating reeds or the tuning forks. Vibrating modulators should be designed for motion amplitudes well within the elastic limit of the material. Corrosion of material used without a suitable protective coating may shift the natural frequency of vibration, with a corresponding second-order effect on alinement.

4.2.3.2 Electronic Scan Stability

In systems with electronic scanning, the index error is directly affected by the null stability of the scanning tube (vidicon or image dissector) and its deflection systems. Null stability can be controlled by attention during design to the following factors:

(1) Temperature-induced shifts
(2) Shock and vibration shifts
(3) Power-supply variations
(4) Tolerance of signal magnitude changes
(5) Stray magnetic fields
(6) Electrostatic-charge build-up

Temperature shift can occur both from dimensional changes and from the use of ferrite cores in the deflection system. The latter should be eliminated from sensitive systems.

Shock and vibration may affect the front electrodes in the image section of an image dissector or the electron-gun-to-cathode relationship in a vidicon. Rugged tubes should be specified, and shake tests should be conducted before commitment to tracker use.

Stray fields readily affect image dissectors. Use of magnetic shielding calls for attention to its spacing from the tube and its tendency to exhibit hysteresis, because hysteresis by itself can cause index shifts. The use of thin, iterated shielding is recommended, along with design proof testing.

Where buildup of electrostatic charge in the image section of image dissectors is observed, with a corresponding effect on index, grounding of the cathode end of the high voltage is recommended.

4.2.3.3 Optical Stability

Elements of the optical system requiring specific attention are those whose positional drift have the greatest effect upon alinement (e.g., objectives, Cassegrain secondary mirror, and folding mirrors). Low-power corrective elements are less critical. The focal length of optical systems offers no inherent clue to their stability. Much depends upon the material, dimensions, and symmetry of their enclosing structure. A computer evaluation of the contribution made by positional errors of each optical element to the optical performance is recommended as a means for determining manufacturing tolerances.

4.3 Design Considerations

4.3.1 Photodetector

Detectors differ greatly in their influence on size, weight, reliability, and cost in meeting a given level of tracker performance. Some of the factors to be considered are compared in table II for those detectors most commonly used in spaceborne applications. Specific data, such as dark noise, quantum efficiency, etc., do not indicate directly the performance of the tracking system or allow a comparison between systems and are therefore not included.

Specific discussions of these and other detectors may be found in references 4, 22, and 26 to 30. Spectral responses of all but the vidicon and CdSe detectors may be found in Appendix B along with a listing of the current responses to specific stars.

The image orthicon, which has a photoemissive detector in combination with the capability of image storage, is also quite appropriate for spaceborne applications where faint stars are to be tracked in low background and where some base stabilization is available. Its bulk and critical operating parameters exclude it from most applications in space.

TABLE II.—*Qualitative Comparison of Photodetectors*

Quality	Photo-multiplier	Image Dissector	Vidicon	Solid-state element
Form	Photoemissive surface in vacuum	Photoemissive surface in vacuum	Photoconductive surface in vacuum	Photoconductive or photovoltaic chip
Color sensitivity	Near UV to near IR with blue dominant	Near UV to near IR with blue dominant	Approximately photopic	Red to near IR
Frequency response limitations (as used)	None in most applications	None in most applications	<10 Hz	Silicon: none CdSe: <100 Hz
Associated modulation or scan	Mechanical modulation	Electronic modulation or scan past aperture plate	Electronic scan of stored image	Mechanical modulation
Advantage	Low internal noise	Lowest internal noise	Background tolerance	Background tolerance
	Simple	Easily offset scan and track	Easily offset scan	Compact

For proper specification and control of photodetector characteristics, it is essential that their individual contributions to performance be quantitatively evaluated. Certain properties, such as spectral response, cathode uniformity, and physical dimension, may have to be specified tightly. Acceptable limits for temperature, microphonics, stray fields, etc., should be determined quantitatively and by test if necessary. If the photodetector is procured as a stock item, modifications or additions to the component may be necessary to meet requirements.

4.3.1.1 Photomultipliers

Photomultiplier tubes have low dark current and relatively low quantum efficiency (0.4 to 20 percent) but high gain (as high as 10^6) and are shot-noise limited and temperature sensitive (ref. 31). Good S/N ratios can be obtained at the tube output, provided background and extraneous light inputs are low, which simplifies subsequent electronics.

The location of the detecting surface inside the photomultiplier requires that external means be used for star modulation. Electrically driven modulators of the vibrating type may be used without concern for wear (ref. 32). Any attempt to relay the focal plane optically onto the photocathode is to be avoided because of the severe variation in tube gain with spot position on the photocathode, and because there is no functional purpose in so doing. The recommended procedure for optical design is to image the entrance aperture onto the photocathode.

4.3.1.2 Image Dissectors

Image dissectors use the same photocathodes as the photomultiplier and are recommended for the same applications. They are especially suited to systems in which mechanical gimbaling is not desired, or where offset star tracking within the FOV is appropriate. The relative ease with which the photoelectron image may be electronically deflected past the internal scanning aperture offers a variety of modulation patterns to be formed anywhere within the working FOV.

The small instantaneous FOV facilitates the suppression of background gradients and reduces internal dark noise. The stellar field must be imaged on the photocathode, requiring careful control by the manufacturer over uniformity of cathode response.

4.3.1.3 Vidicons

The vidicon is especially recommended where high search rate must be achieved against a relatively high background.[7] Its property of photocurrent integration at the faceplate and its small instantaneous FOV as produced by the electron-beam scan, maximize star acquisition against both background and stray-light inputs. Electronic deflection facilitates a scan of the working FOV, and the determination of star position in planar Cartesian coordinates relative to the center of the field.

To obtain the benefit of the noise-integrating feature of the vidicon, the tracker using this detector should be stabilized with respect to the target star so that the star image remains essentially motionless between scans. Gyro stabilization is entirely suitable for the prevention of such image smear because the directions of stars in inertial space are essentially constant. The need for stabilization, however, tends to preclude use of the vidicon for offset tracking in the presence of vehicle attitude variations.

---

[7]With daylight background levels, the scanning rate can be faster by a factor of several hundred than that of a photomultiplier.

Adaptation of the vidicon to spaceborne trackers requires a departure from commercial practice to parameter values empirically verified on star targets in typical backgrounds. If background and scattered light is high, frame time should be limited to avoid background saturation and consequent reduction of incremental sensitivity to stars. Extraneous light also generates coherent noise from hot spots on the photosensitive surface. Current practice requires the storage of hot-spot locations in a computer memory for subsequent elimination of the false star pulses during extraction of star-position data from the video signal.

For low-background conditions, the vidicon holds no advantage over the photoemissive detectors. Thermal noise contributed by the faceplate load resistor and preamplifier completely dominates photon-derived shot noise.

The susceptibility of the vidicon filament to shock and vibration should be considered in terms of both transport and launch environments. Testing under shock has demonstrated a significantly higher survival of the filament when lit. Excitation of the filament throughout launch is therefore recommended.

4.3.1.4 Solid-State Detectors

The silicon photodiode and the cadmium selenide photoconductive cell are representative of the solid-state detectors now finding useful application. For maximum S/N ratio, silicon can be operated in a condition of slight reverse bias, resulting in a high-impedance source suitable for loading into an operational preamplifier.

As a photoconductor, the CdSe detector normally operates in a voltage-biased circuit. Its response time increases inversely with light level to the extent that, for star detection, it is current practice to light-bias the cell with an internal source to reduce the time constant to a practicable level for tracker application.

In comparison with photoemissive surfaces, solid-state detectors exhibit higher internal noise levels but generally have higher quantum efficiencies. As a result, they are recommended for service where background or scattered light is the dominant noise source. These detectors are also recommended for situations in which intense levels of ambient light may accidentally enter the optics. Neither silicon nor CdSe will suffer permanent damage when exposed for brief periods (at least many seconds) to direct sunlight.[8]

Where solid-state detectors are used in trackers requiring high accuracy, a very high ratio of optical aperture to individual cell area (e.g., 10^4) is needed. The resulting small-focal-ratio optics (typically 1.5) require special care in design.

[8]For silicon, the temperature rise should not reach the lead bonding temperature (typically 425° C). For CdSe, a recovery time of up to 10 min is required after exposure to sunlight.

Maximum S/N is obtained when the signal is derived from modulation of the starlight. In current practice, the star image often is moved across one cell or across an array of cells, however, nonuniformity of cell surface and array responsivity should be considered. (Multiple cells provide more FOV and offer means for cancellation of background gradient signal.) To date, this movement is done most efficiently by mechanically introduced deviations in the optical-system LOS. Because of their simplicity and long life, vibrational devices are recommended over frictional mechanical modulators.

4.3.2 Optics

4.3.2.1 Image Formation

A wide variety of optical systems is available for star-tracker design. The final choice depends upon a tradeoff among system accuracy, size, and cost. The requirements placed upon the optics are often shaped by initial system requirements and do not necessarily constitute an optimum or even practicable specification for optical design. To check that the combined effect of these requirements is reasonable and consistent, the guidelines in the following paragraphs are suggested.

The parameters of successful designs, as found in table I, can be referenced as a point of departure.

For perfect, diffraction-limited optics, the angular size of the star image may be approximated by the radial distance to the first minimum beyond the Airy disc, which, in radians, is $1.22\ \lambda/D$ where D is aperture diameter and λ is the dominant wavelength. Even considering the approximation involved, this expression can be used to estimate the theoretically smallest error angle corresponding to full signal. For design purposes, the percent of star energy contained within a given diameter is of more interest. A convenient graph for this purpose is provided in reference 25.

Practicable designs, however, may produce an image size much greater than the diffraction limit. (A typical spot diameter of 0.002 in. is nearly 10 times the diffraction limit for a 12-in. focal length F/4 system.) Designing toward the diffraction limit of the optics rapidly increases its cost and fabrication time and is not recommended unless essential to tracker performance.

In an all-reflective system (e.g., Cassegrain), color correction is complete. Narrow-field designs of light weight and high efficiency are possible. However, the limited number of surfaces available makes high resolution in a wide field (greater than 1°) difficult or impossible.

An all-refractive system requires achromatization for use with broad-band detectors. The longitudinal spread of the color foci is at least 1/1500 of the focal length. Thus, for an F/5 system, the resulting contribution to image blur is nearly 0.5 arcmin. In small field, minute-of-arc systems, simple triplets, and air-spaced doublets can be used to advantage. The number and weight of lens elements can become excessive for wide-field requirements.

Refractive/reflective systems have been found useful for star trackers (modified Cassegrain, Mangin, Maksutov, etc.). The concentric, symmetric form is especially useful when designing for compactness, rigidity, and background tolerance.

For wide-field performance, consideration should be given to designing the area of image modulation or scan to conform exactly to the curvature of the Petzval surface of the optics.

4.3.2.2 Shielding

Light energy directed at the tracker optics from sources beyond the spacecraft can best be suppressed by a shield whose position is fixed with respect to the optical axis. Because of the precision required in locating the shield close to but not in the FOV, the shield should normally be designed as an integral part of the star tracker. The complexity of the shielding structure used depends upon the attenuation required. Three approaches recommended for consideration are illustrated in figure 7. The brightness figure listed beside each type indicates the approximate equivalent in-field brightness produced by a full Sun at the limiting angle θ_s, assuming 1-percent-scattering surfaces. θ_f indicates the working FOV.

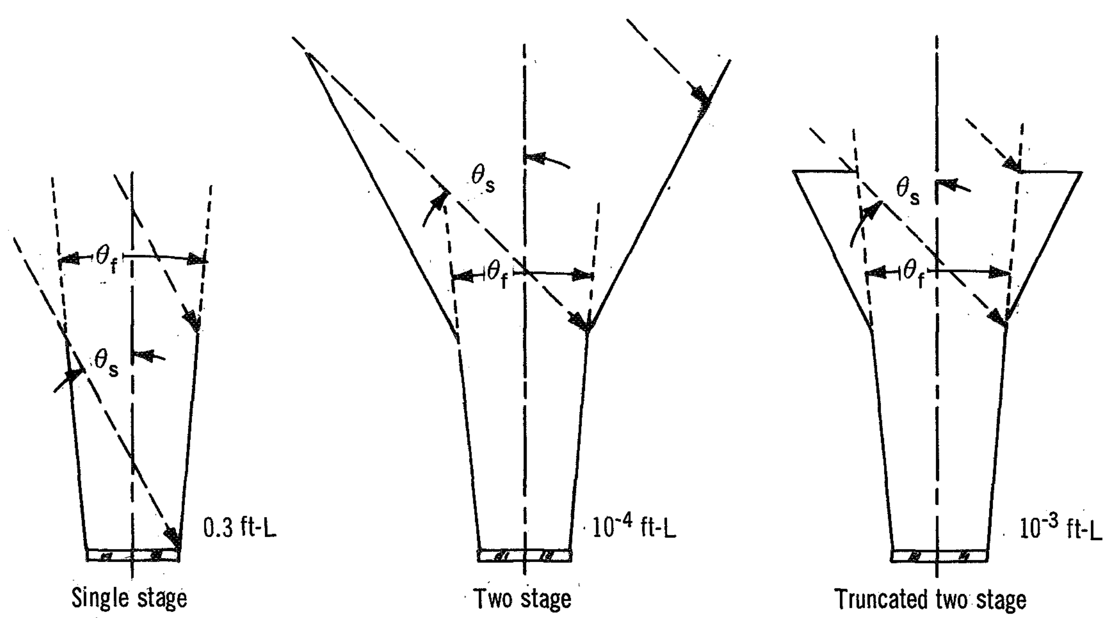

Figure 7.—Stray-light shield geometry.

Two-stage shielding is recommended for systems using the photomultiplier tube if sunlight is to be encountered within 90° of the optical axis. Generally, a one-stage design should be adequate for systems using solid-state or vidicon detectors under similar conditions.

For maximum effectiveness, any optical system and its shield should be kept clean; low-reflectance coatings should be applied to the internal surfaces of the shield and optical housing and to the edges of the glass elements. Commercial preparations with the exact index of refraction are available for the latter.

Masks and aperture stops should be introduced throughout the optical path to trap extrafield light either entering the front or generated within by scattering. (Note, however, that vignetting must be avoided and edge effects considered.)

The preferred location for a shutter is at a region in the optics offering a small aperture for blocking. It should not be located near the focal plane, however, because of the high thermal intensity of the Sun's image formed by the objective. Capping of the entire entrance aperture may be considered as an alternative, although this approach involves a large moving part at an exposed extremity of the equipment, with the possibility of reduced reliability.

4.3.3 Mechanical Design

4.3.3.1 Structure and Materials

The rules for successful mechanical design of the housing, structure, and mechanisms for a spaceborne star tracker are similar to those that apply to guidance platforms, and are distinguished by a concern for high dimensional stability with minimum weight. For trackers, the stringency of this problem is set by star-image size. The effects of temperature, vibration, shock, and aging upon dimensional stability should be such that the resulting index-angle shift is well within the value of star angular diameter. A compact design in which the optics, modulator, and detector are in close proximity is recommended in the interest of structural rigidity, size, and weight.

Materials such as aluminum and beryllium can be advantageously used in structural design because of their high strength-to-weight ratio. Special proprietary alloys such as Meehanite and Tenzaloy deserve mention. All materials should be protected from corrosion if vulnerable in normal atmosphere. (Note that white-room assembly is no guarantee against corrosion.)

Suitability of materials chosen for space hardware merits special attention with regard to the following:

(1) Matching of temperature coefficient of mating materials
(2) Stress relief of structural members, especially for beryllium and aluminum

(3) Choice of paints that do not outgas in orbit. Epoxy-base paints can be pretreated by baking at a temperature (e.g., 200° F) safely below the decomposition level.

4.3.3.2 Thermal Considerations

The thermal interchange between the star tracker, spacecraft, and space environment should be predicted in accordance with currently acceptable thermal models. This step requires knowledge of the tracker power-on duty cycle and the times of exposure toward and away from the Sun. Also, it is necessary to determine the thermal isolation required between tracker and spacecraft, because in some applications, the latter cannot be used as a heat sink. From the standpoint of tracker design, a thermal attachment to a temperature-stable spacecraft is preferred.

Radiant interchange between the tracker and space is best controlled by finishing exposed structural parts with a coating of the correct α/ϵ ratio. If repeated exposure to sunlight is expected, a low value of this ratio is recommended to limit the temperature excursion of the equipment.

4.3.3.3 Lubrication

The smooth, low-friction operation of moving parts such as bearings, brushes, gears, and solenoids can be assured by carefully selecting materials and lubricants. Numerous recommendations in this regard are now compiled (ref. 33).

Low-vapor-pressure oils and greases may be used as fluid lubricants if hermetic or labyrinth seals are employed (ref. 34). This latter technique feeds the lubricant from a wick reservoir to parts isolated from outside vacuum (e.g., 10^{-13} torr) by the small orifices of a labyrinth seal, such that vapor pressure within the seal is above 10^{-4} torr. Current practice also uses high-surface-tension films (fluorinated methacrylate resin) to prevent surface migration of fluid lubricants beyond the enclosed region. Fluid lubricants are especially recommended for preloaded precision bearings.

Solid lubricants are appropriate for certain contacts such as gear teeth or for very-low-temperature bearing startup. In one form, these substances use metallo-organic compounds or molybdenum disulphide and are applied so as to remain bonded to the surfaces (ref. 35). Allowance should be made for the tendency of such lubricants to accumulate. In another form, solid lubricants can be impregnated into electrical brushes for their lubrication. A solid lubricant developed at the Naval Air Materials Laboratory (ref. 36) has been extensively used for gears, solenoids, bearings, etc.

4.3.4 Electronics Design

4.3.4.1 Circuitry

All aspects of normal design practice for spaceborne electronics systems apply to star-tracker circuit design and implementation. Solid-state components and integrated circuits are recommended for use wherever possible. Special attention should be given to circuits involving the detector and preamplifier because of their susceptibility to pickup and microphonics. For photoemissive detectors, electrostatic shielding of the tube is recommended, subject to the precautions of 4.3.4.2. For photodetectors without internal amplification, such as the solid-state variety, it is recommended that the preamplifier be packaged with the detector.

Circuits for the conversion of photodetector signal to pointing-error measures should be designed to minimize loss in S/N ratio. Synchronous detection of the modulated star signal may be used to advantage.

4.3.4.2 Corona Suppression

Photodetectors using electron ballistics, such as photomultipliers, image dissectors, and vidicons, require the application of voltage in the range of 800 to 3000 V to one or more of the electrodes. These circuits are susceptible to corona at partial pressures, and the sensitivity of the photodetector to the accompanying light pulses calls for special measures to prevent their occurrence.

Much experience has been accumulated in the cure and control of this phenomenon, especially as manifested with a photomuliplier tube (ref. 24). Although the application of a grounded shield to the glass envelope quenches visible arcing, it is not recommended for the 1P21. The resulting increase in current flow through the soda-lime glass not only increases dark current, but also develops a permanently increased conductivity at certain points in the tube envelope.

The 1P28, which uses Corning 9741 glass, exhibits higher resistivity by 10^3, with a corresponding reduction of arcing. Still further improvement is possible with a fused silica envelope. With these glasses, successful suppression of corona at the tube envelope can be achieved by the judicious use of potting compounds and insulators.

Another solution lies in grounding the cathode (normally hot) instead of the anode end of the photomultiplier. Special precautions must be taken, however, to prevent the entry of high-voltage-supply ripple into the signal channel.

Other measures for the prevention of circuit arcing and corona include

(1) Use of insulation having low leakage, high voltage-breakdown characteristics, and low outgassing
(2) Sequencing of insulators with conductive interfaces at successively reduced potentials
(3) Location of high-voltage source in close proximity to point of use (e.g., at base of tube)
(4) Elimination of pockets in high-voltage areas where gases may become entrapped at partial pressures

4.4 Alinement, Calibration, and Test

4.4.1 Internal Alinement

Provision for test of internal tracker alinement can be made by designing reference flats or bosses on the outer surfaces of the basic tracker structure. On a strapped-down tracker, this structure may be the casting that holds the optics and modulator or scanner. In the case of a gimbaled tracker, the base supporting the first gimbal trunnion may be used. The reference surfaces should be arranged to constrain the mounting position to one unique angular attitude. Redundant constraints that might distort the tracker structure when bolted in place should be avoided. The use of kinematic mounting principles should be considered (ref. 37).

Alinement between the mounting interface and the effective tracker LOS is best determined by a fixture that presents a mating mount surface and simulated star in known angular relationship to the tracker. For a gimbaled tracker, this test fixture must be provided with at least two axes capable of varying the star/mount relationship throughout a full set of test positions. A flexible shield should be attached between simulator and tracker to permit testing under normal lighting conditions.

4.4.2 Star Sensitivity Calibration

Although the expected level of real-star signal may be estimated by the procedures of section 4.1, a simulation of starlight will be needed for calibration and test of the tracking equipment both at the factory and at user stations in the field. The simulator should consist of a controllable source of collimated light having a known and repeatable irradiance. As with the procedure on real stars, the effective content of simulated starlight is determined for the system under test. This step requires knowledge of the spectral power density of the simulator and the spectral response of the detector.

Many arrangements for star simulation have been used in the calibration of star trackers (refs. 38 and 39). Dissimilarities in flux source, as well as bench setup and procedure have led to repeated difficulty in reconciling differences between simulators, even on the same program. One approach that has received some acceptance uses two setups:

(1) A National Bureau of Standards calibrated quartz-iodine lamp is attenuated by geometry such as that reviewed by Meisenholder (ref. 39) to create a highly calibrated but slightly divergent flux at starlight level. This flux is intercepted by a detector serving as a reference standard, and the response is measured.
(2) An accurate collimator of oversized beam diameter is equipped with similar quartz-iodine source and adjusted until its output flux gives the same reading on the standard detector. The collimator is now calibrated as a star source for testing a complete tracker.

For some applications, the simulation of other celestial bodies such as the Sun (ref. 40), Moon, Earth's limb, or a planet is required. It should be noted, however, that when such simulations are used for stray-light studies, the angular distribution of test flux impinging on the tracker should correspond to the real situation as far as is practicable. Relatively close-range sources, such as sunlit Earth, require strict attention.

4.4.3 Test with Spacecraft

Boresight alinement of the internally alined star tracker to the spacecraft is insured to the extent that the mounting pad has been correctly prealined to the vehicle structure. If the star tracker is to supply vehicle attitude to the order of arcseconds, however, it is recommended that the final boresight position of the tracker with respect to the spacecraft coordinate system be checked by an assembly that presents a reference frame and simulated star to the spacecraft assembly in a fashion analogous to the internal-alinement test fixture discussed in 4.4.1.

On-pad testing may be performed using a star simulator configured to fit over the mounted tracker. The simulator can be preadjusted to present a minimum star and can physically interface with the tracker, provided that suitable reference surfaces and tie points have been provided during tracker design. A light shield should also be provided for this test.

REFERENCES

1. Whitford, A. E.; and Kron, G.: Photoelectric Guiding of Astronomical Telescopes. Rev. Sci. Instr., vol. 8, Mar. 1937, pp. 78-82.

2. Engstrom, Ralph W.: Multiplier Phototube Characteristics; Application to Low Light Levels. Pub. No. ST-356, RCA, June 1947.

3. Greene, Joel: The Celestial Tracker as an Astro Compass. IEEE Trans., vol. ANE-10, no. 3, Sept. 1963, pp. 221-235.

4. Laverty, Norman P.: The Comparative Performance of Electron Tube Photodetectors in Terrestrial and Space Navigation Systems. IEEE Trans., vol. ANE-10, no. 3, Sept. 1963, pp. 194-205.

5. Wichman, W. J.; and Birnbaum, M. M.: Servo System Design for Balloon Star Trackers. Electronics, vol. 34, Sept. 1, 1961, pp. 43-46.

6. Strong, John: Balloon Telescope Optics. Appl. Op., vol. 6, no. 2, Feb. 1967, pp. 179-190

7. Schlesinger, E. R.: Aiming a 3-Ton Telescope Hanging from Balloon. Electronics, vol. 36, Feb. 8, 1963, pp. 47-51.

8. Gehrels, Thomas: Ultraviolet Polarimetry Using High Altitude Balloons. Appl. Op., vol. 6, no. 2, Feb. 1967, pp. 231-233.

9. Anon.: Mariner Venus 67 Final Project Report. Vol. II, Mid-course Maneuver Through End of Mission. JPL Tech. Rept. 32-1203, May 1969.

10. Meisenholder, Gerald W.; and Davis, Edgar S.: The Mariner IV Canopus Sensor. 16th International Aeronautical Congress, 1965. Guidance and Control Vol., pp. 83-103.

11. Anon.: Mariner Venus 67 Guidance and Control System. JPL Tech. Rept. 32-1258, July 1968.

12. Anon.: Surveyor Final Engineering Report. Vol. II, Systems Design. SSD 88027, Hughes Aircraft Co., June 1968, pp. 4-53–4-76.

13. Lansing, Jack C., Jr.: Calibration and Spaceborne Performance of the Surveyor Spacecraft Star Sensor. J. Spacecraft Rockets, vol. 5, no. 1, Jan. 1968, pp. 84-89.

14. Fosth, Douglas; and Mitchell, Warren I.: Lunar Orbiter Attitude Control System. AIAA reprint 67-533.

15. Anon.: Analysis of Flight Problems—Lunar Orbiter. NASA CR-66583, 1968.

16. Meltzer, Irving M.: Vidicon Stellar Sensor. Technical News Bull., Aerospace Group, General Precision, Inc., 1966.

17. Schwarzschild, Martin; and Schwarzchild, Barbara: Balloon Astronomy. Sci. Am., vol. 200, no. 5, May 1959, pp. 52-59.

18. Mintz, L. J.; and Jackson, B. W.: The Goddard Experimental Package. IEEE Trans., Aerospace and Electronic Systems Issue, vol. AES-5, no. 2, Mar. 1969, pp. 253-260.

19. Anon.: Micrometeorite Shower Disables Mariner 4. Aviation Week, vol. 88, no. 1, Jan. 1, 1968, p. 22.

20. Naavi, A. M.; and Levy, R. J.: Some Astronomical and Geophysical Considerations for Space Navigation. IEEE Trans., vol. ANE-10, no. 3, Sept. 1963, pp. 154-170.

21. Anon.: The American Ephemeris and Nautical Almanac for the Year 1969, U.S. Government Printing Office.

22. Quasius, Glen; and McCanless, Floyd: Star Trackers and System Design. Spartan Books., Inc., 1966.

23. Bender, Allen G.; Wilson, Robert E.: Convenience Tables of Outside Atmosphere Sky Brightness. NASA GSFC Rept. X-732-69-96, Mar. 1969.

24. Street, H. W.; Boyle, J. C.; Maier, E. J.; Plitt, K. F.; Thienel, C. E.; and Block, A. F.: High Voltage Breakdown Problems in Scientific Satellites. NASA Goddard Space Flight Center Report X-300-66-41, 1966.

25. Abate, John E.: Star Tracking and Scanning Systems, Their Performance and Parametric Design. IEEE Trans., vol. ANE-10, no. 3, Sept. 1963, pp. 171-181.

26. Schuck, Walter H.: Vidicon Star Tracker. Appl. Op., vol. 5, no. 4, Apr. 1966, pp. 489-496.

27. Schleuter, P.: Photomultiplier Tubes for Satellite Instrumentation. Appl. Op., vol. 6, no. 2, Feb. 1967, pp. 239-244.

28. Eberhardt, E. H.: Threshold Sensitivity and Noise Ratings of Multiplier Phototubes. Appl. Op., vol. 6, no. 2, Feb. 1967, pp. 251-256.

29. Rome, Martin; Fleck, H. G.; and Hines, D. G.: The Quadrant Multiplier Phototube, A New Star-Tracker Sensor. Appl. Op., vol. 3 no. 6, June 1964, pp. 691-695.

30. Barnes, John W.; and Walker, Burt: Some Recent Advances in the Development of Solid State Celestial Trackers. Navigation, vol. 13, no. 4, Winter 1966-67, pp. 367-381.

31. Young, Andrew T.: Temperature Effects in Photomultipliers and Astronomical Photometry. Appl. Op., vol. 2, no. 1, Jan. 1963, pp. 51-60.

32. Zuckerbraun, J.: High Reliability Scanners for Stellar Navigation. Electronics, vol. 35, May 11, 1962, pp. 82-85.

33. Clauss, Francis J.: Lubrication as Part of Total Design. Proceedings of the 2nd Aerospace Mechanisms Symposium, NASA TM 33-355, Aug. 1967, p. 121.

34. Silversher, H. I.: Controlled Leakage Sealing of Bearings for Fluid Lubrication in a Space Vacuum Environment. Proceedings of the 3rd Aerospace Mechanisms Symposium, NASA TM 33-382, Oct. 1968, p. 93.

35. Perrin, B. J.; and Mayer, R. M.: Lubrication of DC Motors, Slip Rings, Bearings and Gears for Long Life Space Applications. Proceedings of the 3rd Aerospace Mechanisms Symposium, NASA TM 33-382, Oct. 1968, p. 65.

36. Anon.: Lubricant, Solid Film Extreme Environment, MIL-L-81329(2), Jan. 1967.

37. Bateman, T. A.: Adjustable Mirron Mount Design Using Kinematic Principles. AD 65-3695-CFSTI, Ministry of Technology, England.

38. Draper, Lawrence T.: Star Tracker Calibration. NASA TN D-4594, 1968.

39. Meisenholder, Gerald W.: A Practical Method for Sensor Absolute Calibration. Appl. Op., vol. 5, no. 4, Apr. 1966, pp. 533-536.

40. Fain, D. L.: Design Considerations for Precision Solar Simulation. Appl. Op., vol. 3, no. 12, Dec. 1964, pp. 1389-1395.

APPENDIX A
GLOSSARY

Acquisition field of view.—The angular field covered by motion of the instantaneous field of view during the acquisition mode.

Acquisition mode.—The mode of operation that provides for the detection of a star when present in the field of view and which compares the star with specific acceptance criteria.

Acquisition probability.—The probability that a star-tracker system will develop a presence signal on a given star in an assigned period of time.

Acquisition time.—The time allotted for the recognition of an acceptable star when present in the acquisition FOV.

Coherent noise.—Noise that has some form of regularity in its occurrence.

Detector response.—Any quantitative expression of the electrical output signal yield of the detector for a given received optical input power.

Electronic scanning (or *Scanning*).—A systematic piecewise examination of the electronic status or output of a detector area to determine the presence and location of one or more star images on the detector. Scanning is performed in the vidicon and image dissector by electrostatic or electromagnetic deflection. Other techniques, such as light-beam scanning or electronic circuit switching to elements of an array, are possible. Scanning does not imply modulation.

Index error.—The effective sum of the infrequent or slowly changing errors that shift the alinement between the star sensor's pointing axis and its mount.

Instantaneous field of view.—That portion of the working field seen by the star tracker at any instant of time. Its size and instantaneous direction are governed by the type of star-modulation system.

Maximum gimbal angle.—The maximum mechanical angle through which the working FOV can be moved with respect to the fixed base of the star tracker. Gimbal angle may be preset or may move as a part of the tracking loop.

Modulation.—The periodic interruption of starlight arriving at the photodetector. This form of modulation may be effected by obscuration or motion of the image, but in all cases, the detector output should change in proportion to the change in intercepted star energy.

Noise.—Spurious and unintended disturbances that tend to mask or obscure the signal developed by the detector.

Noise equivalent angle.—The value of star-tracker error angle at which the resulting error signal equals the rms random noise.

Operational accuracy.—The angular difference between the star direction as represented at the tracker output and the true star direction. Operational accuracy includes both random and systematic or index-error effects as expected in the final operational environment.

Optical aperture.—The dimension of the entrance pupil of the collecting optics, expressed in terms of either diameter or area. When obstructions such as a concentric secondary mirror are accounted for by subtraction, the remaining aperture is termed *effective aperture.*

Optical resolution.—The angle subtended by two points or lines that are just far enough apart to permit them to be distinguished as separate. The ability of an optical device to resolve two points or lines is called resolving power and quantitatively is inversely proportional to the limiting optical resolution as defined.

Photodetector (or *Detector*).—That component of a star tracker which converts the collected star irradiant power to an electrical signal.

Probability of false acquisition.—The probability that a star-tracker system will develop a presence signal without a star in the FOV.

Random error.—The error in star-tracker output signal that appears randomly distributed with time. Random error is usually expressed in terms of the standard deviation σ.

Random noise.—Noise definable in amplitude and time only in terms of statistical model, such as a Gaussian distribution.

Resolution.—The smallest increment of measure that is detectable, expressible in terms of either the increment or its percentage of the full span of measure.

Rise time.—The time required for a signal to go from 10 percent to 90 percent of its maximum value.

Search area.—The area of sky to be explored for the presence of a star. This area may exceed the working field of view if gimbals or other means are used for redirecting the working FOV.

Search time.—The time required to explore the search field for the presence of a star. Search time is thus greater than acquisition time by the number of times the acquisition field is mapped into the search field.

Shot noise.—Noise caused by random availability of electrons constituting current flow in the signal channel. Current flow may be induced by thermionic emission, photoelectric emission, or photo-generated carriers in a semi conductor.

Star magnitude.—A logarithmic scale of brightness comparison for stars when sensed by a given detector. For each unit increase in magnitude, the apparent brightness (as judged by detector output) is decreased by the 1/5th root of 100, or by the factor 1/2.51. Hence, $M = -5/2 \log B_1/B_0$, where M = magnitude value for star brightness B_1 relative to reference brightness B_0.

Star tracker.—A system capable of determining automatically the direction of a star as a physical entity in the measurable vicinity of a coordinate system. In support of the tracking function, a star tracker may also search, acquire, and measure pointing errors and angles.

Track field of view.—The angular field covered by motion of the instantaneous field of view during the tracking mode.

Tracking bandwidth (B).—The bandwidth in which the tracker output information is delivered at the system interface.

Tracking mode.—The mode of operation when star pointing-error signals are generated. With some designs, this mode also includes an electronic or mechanical response to the error signal so as to develop angular measures of star direction.

Working field of view.—The total solid angle of view directly presented by the optics to the detector for targets at infinity.

APPENDIX B
STELLAR PHOTOMETRIC DATA FOR VARIOUS PHOTOCATHODE MATERIALS[1]

There presently exists in the literature sufficiently accurate narrow-band filter photometric stellar data for approximately 1000 of the brightest stars[2] to allow the computation of the radiant energy of these stars per square centimeter of effective aperture. In addition to the photometric measurements obtained using an RCA 1P21, S-4 photosensitive surface, recent narrow-band photometers[3] using an RCA 7102, S-1 photosensitive surface has allowed the energy computations to be extended to the new infrared wavelengths. We have computed the radiant energy falling on the Earth from outside the Earth's atmosphere in terms of amperes per square centimeter of telescope aperture for the S-1, S-4, S-11, S-17, and S-20 photomultiplier tubes[4] and bialkali photocathodes,[5] and for the silicon detector.[6] The computations are based directly upon precise narrow-band filter photometry measurements of individual stars: therefore, the usual assumptions involving bolometric corrections or star temperature[7] are advantageously disregarded. The compilation of results for nearly 1000 stars[8] has been condensed in table B-I to include the 57 navigational stars.[9] In addition to

---

[1]F. F. Forbes and R. I. Mitchell, Lunar and Planetary Laboratory, University of Arizona, Tucson, Arizona.

[2]See H. L. Johnson, R. I. Mitchell, and A. S. Latham, Eight Color Narrow-Band Photometry of 985 Bright Stars, Vol. 6 of Communications, Lunar and Planetary Laboratory, Part 2, No. 92, for a description of the eight-color photometric system used, filter characteristics, and eight-color photometry for 985 stars.

[3]H. L. Johnson and R. I. Mitchell, 13-color photometry as proposed in reference 1. (Unpublished data, University of Arizona.)

[4]Typical Absolute Spectral Response Characteristics of Photomissive Devices, chart published by ITT Industrial Laboratories, Fort Wayne, Indiana.

[5]RCA 4523, RCA Information Sheet on Electronic Components & Devices, Harrison, N.J.

[6]Hewlett-Packard Technical Data Publication, July 15, 1967, for HP 42 Series PIN Photodiode.

[7]See G. Quasius and F. McCanless, Star Trackers and Systems Design, ch. 1. MacMillan & Co. Ltd., London, 1966.

[8]R. I. Mitchell and H. L. Johnson, Communications, Lunar and Planetary Laboratory, Vol. 8, Part 1, Feb. 24, 1969, University of Arizona.

[9]The Air Almanac, U.S. Government Printing Office (January-April), 1969.

TABLE B-I.–*Response in Amperes Per Square Centimeter of Telescope Aperture*

Nav No.	B.S. No.	Const.	S.H.A.	Dec.	MK Spect.	V	S-1	S-4	S-11	S-17	S-20	Bialkali	Silicon
18	2491	α CMa	259° 03′	-16° 40′	A1 V	-1.46	0.994E-14	0.181E-12	0.224E-12	0.400E-12	0.315E-12	0.281E-12	0.185E-11
17	2326	α Car	264 11	-52 41	F0 Ib-II	-0.75	0.542E-14	0.832E-13	0.102E-12	0.186E-12	0.150E-12	0.127E-12	0.107E-11
38	5459D	α Cen	140 37	-60 42	G2 V	-0.28	0.349E-14	0.349E-13	0.444E-13	0.813E-13	0.709E-13	0.526E-13	0.758E-12
37	5340	α Boo	146 26	19 20	K2 IIIp	-0.05	0.395E-14	0.198E-13	0.268E-13	0.493E-13	0.483E-13	0.289E-13	0.869E-12
49	7001	α Lyr	81 02	38 45	A0 V	0.03	0.254E-14	0.459E-13	0.569E-13	0.101E-12	0.803E-13	0.713E-13	0.483E-12
12	1708	α Aur	281 24	45 58	G8 III	0.08	0.278E-14	0.254E-13	0.318E-13	0.581E-13	0.514E-13	0.368E-13	0.606E-12
11	1713	β Ori	281 44	- 8 14	B8 Ia	0.13	0.313E-14	0.514E-13	0.625E-13	0.114E-12	0.861E-13	0.800E-13	0.452E-12
20	2943	α CMi	245 34	5 18	F5 IV-V	0.37	0.199E-14	0.254E-13	0.319E-13	0.579E-13	0.477E-13	0.388E-13	0.402E-12
5	472	α Eri	335 52	-57 24	B5 IV	0.47	0.231E-14	0.418E-13	0.505E-13	0.927E-13	0.691E-13	0.648E-13	0.335E-12
35	5267	β Cen	149 36	-60 13	B1 II	0.62	0.266E-14	0.467E-13	0.560E-13	0.104E-12	0.745E-13	0.728E-13	0.298E-12
16	2061V	α Ori	271 37	7 24	M2 Iab	0.42	0.573E-14	0.924E-14	0.130E-13	0.242E-13	0.308E-13	0.132E-13	0.116E-11
51	7557	α Aql	62 41	8 47	A7 IV-V	0.76	0.132E-14	0.203E-13	0.254E-13	0.457E-13	0.369E-13	0.314E-13	0.263E-12
30	4730D	α Cru	173 47	-62 56	B1 IV	0.76	0.243E-14	0.417E-13	0.500E-13	0.929E-13	0.667E-13	0.651E-13	0.276E-12
10	1457V	α Tau	291 28	16 27	K5 III	0.86	0.226E-14	0.675E-14	0.942E-14	0.174E-13	0.191E-13	0.970E-14	0.480E-12
42	6134V	α Sco	113 07	-26 22	M2 I	0.91	0.331E-14	0.607E-14	0.845E-14	0.158E-13	0.193E-13	0.870E-14	0.675E-12
33	5056V	α Vir	159 06	-11 00	B1 V	0.97	0.185E-14	0.320E-13	0.391E-13	0.722E-13	0.513E-13	0.499E-13	0.207E-12
21	2990	β Gem	244 08	28 06	K0 III	1.14	0.108E-14	0.762E-14	0.101E-13	0.185E-13	0.171E-13	0.112E-13	0.239E-12
56	8728	α PsA	16 01	-29 47	A3 V	1.16	0.869E-15	0.150E-13	0.185E-13	0.336E-13	0.267E-13	0.231E-13	0.170E-12
53	7924	α Cyg	49 55	45 10	A2 Ia	1.25	0.909E-15	0.145E-13	0.177E-13	0.317E-13	0.254E-13	0.226E-13	0.163E-12
26	3982	α Leo	208 19	12 07	B7 V	1.35	0.880E-15	0.159E-13	0.195E-13	0.352E-13	0.269E-13	0.248E-13	0.140E-12
19	2618	ε CMa	255 39	-28 56	B2 II	1.50	0.111E-14	0.197E-13	0.237E-13	0.440E-13	0.317E-13	0.307E-13	0.130E-12
31	4763V	γ Cru	172 38	-56 56	M3 II	1.63	0.207E-14	0.338E-14	0.466E-14	0.864E-14	0.107E-13	0.489E-14	0.417E-12
45	6527	λ Sco	97 07	-37 05	B1 V	1.63	0.955E-15	0.173E-13	0.208E-13	0.386E-13	0.278E-13	0.270E-13	0.112E-12
13	1790	γ Ori	279 08	6 19	B2 III	1.64	0.974E-15	0.170E-13	0.207E-13	0.382E-13	0.274E-13	0.266E-13	0.114E-12
14	1791	β Tau	278 55	28 35	B7 III	1.65	0.726E-15	0.130E-13	0.159E-13	0.289E-13	0.218E-13	0.203E-13	0.108E-12
24	3685	β Car	221 47	-69 35	A1 IV	1.68	0.566E-15	0.100E-13	0.123E-13	0.223E-13	0.176E-13	0.155E-13	0.108E-12
15	1903V	ε Ori	276 20	- 1 13	B0 Ia	1.69	0.959E-15	0.159E-13	0.194E-13	0.361E-13	0.256E-13	0.248E-13	0.106E-12
55	8425	α Gru	28 26	-47 07	B5 V	1.74	0.668E-15	0.123E-13	0.148E-13	0.273E-13	0.205E-13	0.190E-13	0.101E-12
32	4905	ε UMa	166 49	56 07	A0 p	1.77	0.519E-15	0.946E-14	0.116E-13	0.207E-13	0.164E-13	0.147E-13	0.981E-13
27	4301	α UMa	194 32	61 55	K0 III	1.79	0.601E-15	0.392E-14	0.523E-14	0.961E-14	0.900E-14	0.578E-14	0.133E-12
9	1017	α Per	309 29	49 45	F5 Ib	1.79	0.513E-15	0.600E-14	0.762E-14	0.137E-13	0.116E-13	0.915E-14	0.110E-12
22	3307V	ε Car	234 32	-59 25	K0 p	1.86	0.429E-15	0.359E-14	0.468E-14	0.872E-14	0.764E-14	0.530E-14	0.947E-13
48	6879	ε Sgr	84 28	-34 24	A0 V	1.85	0.506E-15	0.921E-14	0.112E-13	0.204E-13	0.158E-13	0.142E-13	0.910E-13
34	5191	τ UMa	153 25	49 28	B3 V	1.86	0.672E-15	0.120E-13	0.147E-13	0.269E-13	0.197E-13	0.187E-13	0.903E-13
43	6217	α TrA	108 39	-68 58	K4 III	1.92	0.612E-15	0.277E-14	0.373E-14	0.692E-14	0.711E-14	0.402E-14	0.135E-12
52	7790	α Pav	54 12	-56 50	B3 IV	1.94	0.651E-15	0.118E-13	0.143E-13	0.263E-13	0.193E-13	0.184E-13	0.860E-13
25	3748	α Hya	218 29	- 8 31	K4 III	1.97	0.618E-15	0.258E-14	0.357E-14	0.661E-14	0.682E-14	0.373E-14	0.135E-12
6	617	α Ari	328 39	23 19	K2 III	2.00	0.520E-15	0.304E-14	0.409E-14	0.751E-14	0.720E-14	0.446E-14	0.115E-12
4	188	β Cet	349 30	-18 09	K1 III	2.02	0.450E-15	0.307E-14	0.408E-14	0.749E-14	0.698E-14	0.453E-14	0.100E-12
36	5288	θ Cen	148 47	-36 13	K0 III-IV	2.06	0.462E-15	0.317E-14	0.413E-14	0.758E-14	0.714E-14	0.471E-14	0.103E-12
1	15	α And	358 19	28 55	B9 p	2.06	0.496E-15	0.885E-14	0.108E-13	0.196E-13	0.148E-13	0.137E-13	0.760E-13
40	5563	β UMi	137 18	74 17	K4 III	2.08	0.607E-15	0.236E-14	0.327E-14	0.605E-14	0.634E-14	0.340E-14	0.132E-12
46	6556	α Oph	96 38	12 35	A5 III	2.07	0.375E-15	0.610E-14	0.761E-14	0.136E-13	0.109E-13	0.941E-14	0.749E-13
50	7121	σ Sgr	76 40	-26 20	B2 V	2.03	0.617E-15	0.113E-13	0.135E-13	0.250E-13	0.183E-13	0.175E-13	0.790E-13
28	4534	β Leo	183 07	14 45	A3 V	2.14	0.369E-15	0.631E-14	0.785E-14	0.140E-13	0.112E-13	0.974E-14	0.721E-13
23	3634	λ Vel	223 17	-43 19	K5 Ib	2.21	0.662E-15	0.192E-14	0.264E-14	0.491E-14	0.548E-14	0.276E-14	0.140E-12
3	168	α Cas	350 19	56 22	K0 II-III	2.23	0.403E-15	0.244E-14	0.329E-14	0.606E-14	0.577E-14	0.357E-14	0.902E-13
47	6705	γ Dra	91 02	51 29	K5 III	2.22	0.592E-15	0.198E-14	0.275E-14	0.511E-14	0.550E-14	0.285E-14	0.126E-12
41	5793V	α CrB	126 39	26 49	A0 V	2.24	0.350E-15	0.639E-14	0.791E-14	0.141E-13	0.110E-13	0.993E-14	0.649E-13
2	99	α Phe	353 49	-42 29	K0 III	2.40	0.355E-15	0.220E-14	0.288E-14	0.531E-14	0.507E-14	0.325E-14	0.786E-13
54	8308	ε Peg	34 20	9 44	K2 Ib	2.39	0.425E-15	0.169E-14	0.236E-14	0.438E-14	0.458E-14	0.244E-14	0.932E-13
44	6378D	η Oph	102 51	-15 41	A2.5 V	2.42	0.268E-15	0.469E-14	0.584E-14	0.104E-13	0.831E-14	0.726E-14	0.525E-13
57	8781	α Peg	14 12	15 02	B9.5 III	2.48	0.271E-15	0.494E-14	0.611E-14	0.108E-13	0.859E-15	0.769E-14	0.502E-13
8	911	α Cet	314 50	3 58	M2 III	2.53	0.621E-15	0.144E-14	0.201E-14	0.375E-14	0.430E-14	0.206E-14	0.128E-12
29	4662	γ Crv	176 27	-17 22	B8 III	2.58	0.293E-15	0.528E-14	0.647E-14	0.116E-13	0.893E-14	0.823E-14	0.471E-13
39	5531	α Lib	137 42	-15 55	A m	2.75	0.202E-15	0.332E-14	0.414E-14	0.742E-14	0.596E-14	0.513E-14	0.402E-13
7	897D	θ Eri	315 44	-40 26	A3 V	2.91	0.175E-15	0.290E-14	0.357E-14	0.648E-14	0.519E-14	0.445E-14	0.350E-13

the navigational star number, these tables list the bright star catalog number (B.S.),[10] common constellation name, V magnitude,[11] sidereal hour angle (S.H.A.), declination (DEC), Morgan Keenan spectral type (MK), and detector responses in amperes per square centimeter of telescope aperture. Under the bright star catalog number column, the notations D and V after some star numbers designate the following: D designates two stars observed together that differed by less than 5 mag in brightness; V designates star variability where there is observed brightness variation of greater than 10 percent.

The detector responses for stars south of declination $-20°$ were estimated from sources[12,13] other than notes 1 and 2.

The detector response is given by

$$\int_{0.28}^{1.20} R(\lambda)\, H(\lambda)\, d\lambda$$

where $R(\lambda)$ is the spectral energy distribution of a star interpolated and extrapolated from the 13-color narrow-band system, and $H(\lambda)$ is the monochromatic detector response [(amp/W) λ]. The integration is carried out by Simpson's rule over points interpolated for each 200 Å.

Figure B-I consists of graphs of the spectral sensitivities used in the calculations.

---

[10]D. Hoffleit, Catalogue of Bright Stars, Yale University Observatory, third revised edition, 1964.

[11]The V magnitude was taken from H. L. Johnson, R. I. Mitchell, B. Iriarte, and W. Z. Wisniewski, UBVRIJKL Photometry of the Bright Stars, Communications, Lunar and Planetary Laboratory, No. 63, 1966.

[12]Cousins, Mean Magnitudes, and Colours of Bright Stars South of +10° Declination, Mimeograph, Royal Observatory, Cape of Good Hope, 1967.

[13]E. E. Mendoza, Bull. Ton. y Tac., Vol. 4, 1967, 106.

Additional Reading–

Allen, C. W., *Astrophysical Quantities*, University of London, 2nd Ed., 1963.
Flink, J. H., *Star Identification by Optical Radiation Analysis*, IEEE Transactions in Aerospace and Navigational Electronics, Vol. ANE-10, Sept. 1963, pp. 212-221.
Hiltner, W. A. ed., *Astronomical Techniques*, The University of Chicago Press, Chicago, 1962.

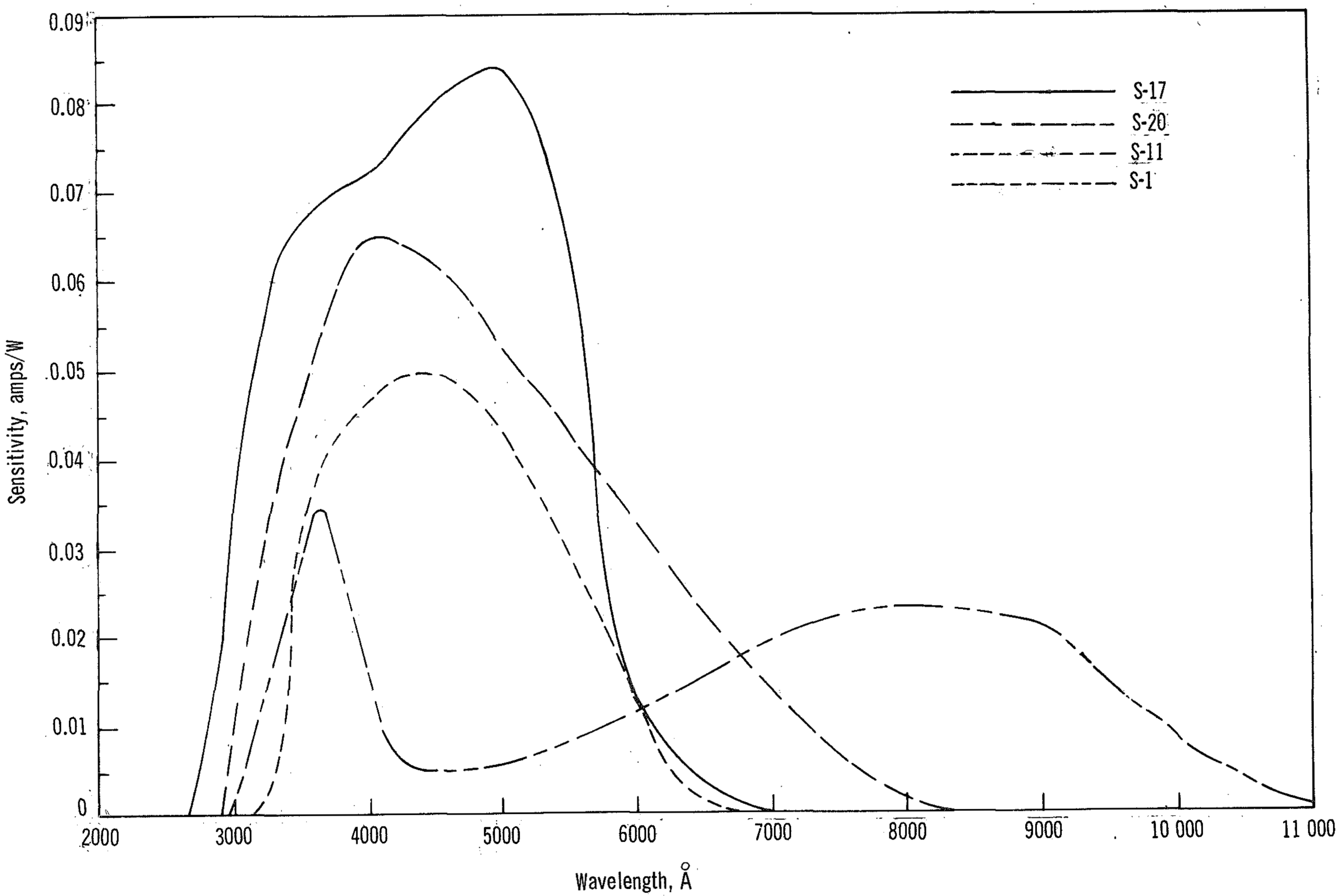
S-17
S-20
S-11
S-1
Sensitivity, amps/W
0.09
0.08
0.07
0.06
0.05
0.04
0.03
0.02
0.01
0
2000
3000
4000
5000
6000
7000
8000
9000
10 000
11 000
Wavelength, Å

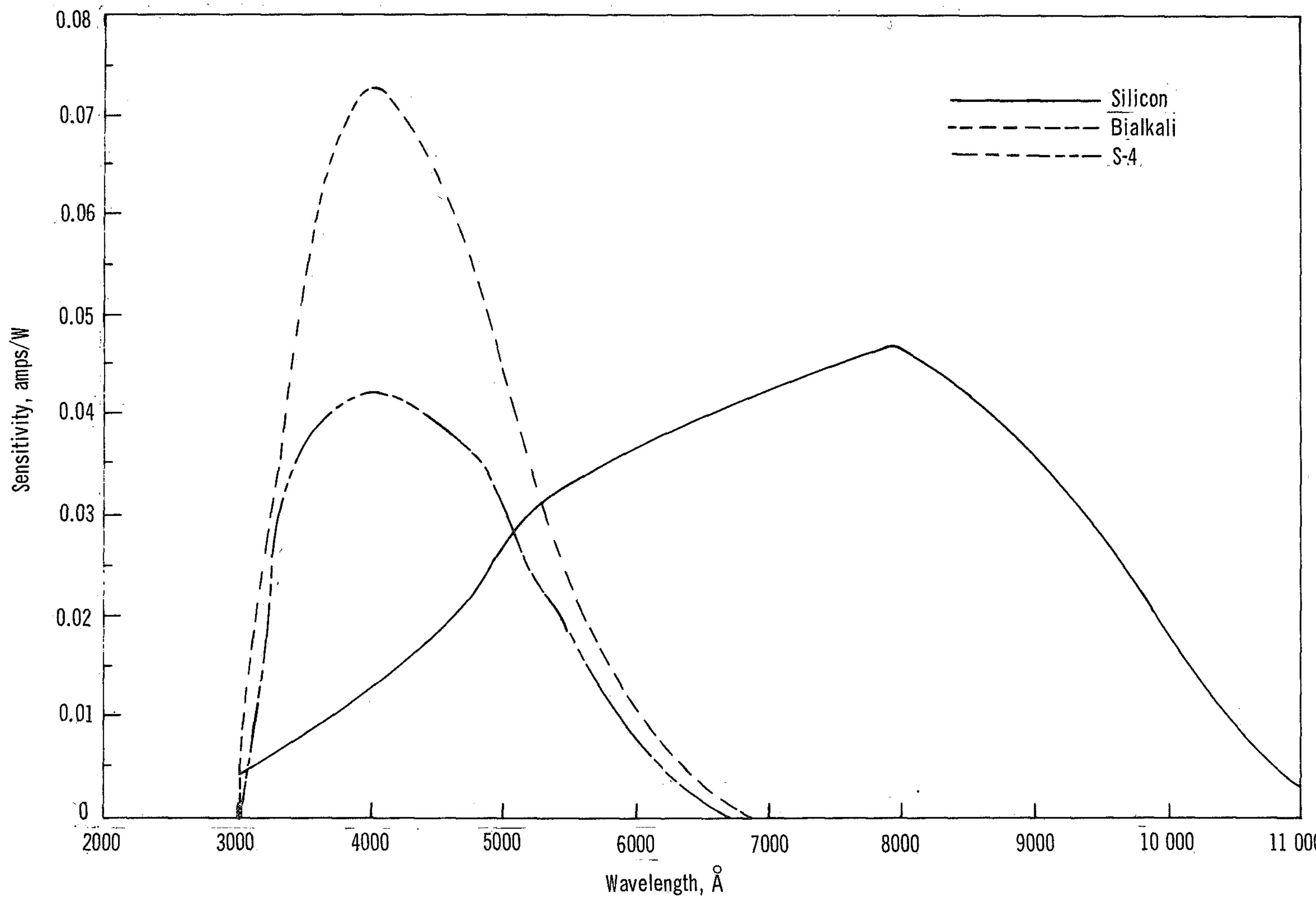

Figure B-1.—Spectral response of selected photodetectors.

APPENDIX C
SIGNAL AND NOISE EQUATIONS

Signal Level: All Photodetectors

$$P_s = H_s A_e$$

where

P_s = effective star power at the sensor, in watts
H_s = effective star power, in watts per unit area, at the sensor wavelength
A_e = effective telescope area (taking into account all the efficiencies)

$$I_s = P_s S E_s$$

where

I_s = signal current
S = sensor response, in amps per watt, at the point of photon conversion
E_s = efficiency of the scanning system

Noise Level

Photomultipliers and Image Dissectors

$$I_n{}^2 = 2e\left(I_s + I_d + I_b\right)B\frac{k}{k-1}k^{2N}$$

where

I_n = rms noise current at the output
e = charge at an electron = 1.6×10^{-19} C
I_s = average signal current

I_d = average cathode dark current picked up by photomultiplier section (refer to catalog data)

I_b = average total background current due to direct background and scattered light

B = bandwidth

k = secondary emission stage gain

N = number of stages

Note: $I_b = FA_e VSE_s$

where F = effective background brightness from all sources, expressed as watts per unit area per unit solid angle.

V = instantaneous field of view in steradians.

Solid-State Sensors

$$I_n^2 = \frac{4KTB}{R_t} + 2e\left(I_s + 2I_0 + I_b\right)B$$

where

I_n = rms noise current

K = Boltzman's constant = 1.38×10^{-23} J/°K

T = temperature of resistors in °K

B = bandwidth

R_t = shot noise equivalent resistance of the input amplifier

e = charge of an electron = 1.6×10^{-19} C

I_s = average signal current

I_0 = average leakage current

I_b = average total background current due to direct background and scattered light

Vidicon

$$I_n^2 = 4KTB\left(\frac{1}{R_L} + \frac{R_{eq}}{R_L^2} + \frac{4\pi^2 C_s^2 R_{eq} B^2}{3}\right) + 2e\left(I_s + I_b + I_d\right)B$$

where

K = Boltzman's constant

T = ambient temperature in °K

R_L = load resistance

R_{eq} = equivalent noise resistor at the preamplifier

C_s = shunt capacitance across preamplifier output

NASA SPACE VEHICLE DESIGN CRITERIA MONOGRAPHS ISSUED TO DATE

SP-8001 (Structures)	Buffeting During Launch and Exit, May 1964
SP-8002 (Structures)	Flight-Loads Measurements During Launch and Exit, December 1964
SP-8003 (Structures)	Flutter, Buzz, and Divergence, July 1964
SP-8004 (Structures)	Panel Flutter, May 1965
SP-8005 (Environment)	Solar Electromagnetic Radiation, June 1965
SP-8006 (Structures)	Local Steady Aerodynamic Loads During Launch and Exit, May 1965
SP-8007 (Structures)	Buckling of Thin-Walled Circular Cylinders, revised August 1968
SP-8008 (Structures)	Prelaunch Ground Wind Loads, November 1965
SP-8009 (Structures)	Propellant Slosh Loads, August 1968
SP-8010 (Environment)	Models of Mars Atmosphere (1967), May 1968
SP-8011 (Environment)	Models of Venus Atmosphere (1968), December 1968
SP-8012 (Structures)	Natural Vibration Modal Analysis, September 1968
SP-8013 (Environment)	Meteoroid Environment Model–1969 (Near Earth to Lunar Surface), March 1969
SP-8014 (Structures)	Entry Thermal Protection, August 1968
SP-8015 (Guidance and Control)	Guidance and Navigation for Entry Vehicles, November 1968
SP-8016 (Guidance and Control)	Effects of Structural Flexibility on Spacecraft Control Systems, April 1969
SP-8017 (Environment)	Magnetic Fields–Earth and Extraterrestrial, March 1969
SP-8018 (Guidance and Control)	Spacecraft Magnetic Torques, March 1969

SP-8019 (Structures)	Buckling of Thin-Walled Truncated Cones, September 1968
SP-8020 (Environment)	Mars Surface Models (1968), May 1969
SP-8021 (Environment)	Models of Earth's Atmosphere (120 to 1000 km), May 1969
SP-8023 (Environment)	Lunar Surface Models, May 1969
SP-8024 (Guidance and Control)	Spacecraft Gravitational Torques, May 1969
SP-8025 (Chemical Propulsion)	Solid Rocket Motor Metal Cases, April 1970
SP-8027 (Guidance and Control)	Spacecraft Radiation Torques, October 1969
SP-8028 (Guidance and Control)	Entry Vehicle Control, November 1969
SP-8029 (Structures)	Aerodynamic and Rocket-Exhaust Heating During Launch and Ascent, May 1969
SP-8031 (Structures)	Slosh Suppression, May 1969
SP-8032 (Structures)	Buckling of Thin-Walled Doubly Curved Shells, August 1969
SP-8033 (Guidance and Control)	Spacecraft Earth Horizon Sensors, December 1969
SP-8034 (Guidance and Control)	Spacecraft Mass Expulsion Torques, December 1969
SP-8035 (Structures)	Wind Loads During Ascent, June 1970

NASA-Langley, 1970 —— 32

NATIONAL AERONAUTICS AND SPACE ADMINISTRATION
WASHINGTON, D. C. 20546

OFFICIAL BUSINESS

FIRST CLASS MAIL

POSTAGE AND FEES PAID
NATIONAL AERONAUTICS AND
SPACE ADMINISTRATION

POSTMASTER: If Undeliverable (Section 158 Postal Manual) Do Not Return